Blood-treatment of Lyme borreliae demonstrates the mechanism of CspZ-mediated complement evasion to promote systemic infection in vertebrate hosts.

Ashley L. Marcinkiewicz[1], Alan P. Dupuis, II[1], Maxime Zamba-Campero[1†], Nancy Nowak[2], Peter Kraiczy[3], Sanjay Ram[2], Laura D. Kramer[1,4], and Yi-Pin Lin[1,4]*

[1]Division of Infectious Diseases, Wadsworth Center, New York State Department of Health, Albany, NY, USA. [2]Division of Infectious Diseases and Immunology, University of Massachusetts Medical School, Worcester, MA, USA. [3]Institute of Medical Microbiology and Infection Control, University Hospital of Frankfurt, Frankfurt, Germany. [4]Department of Biomedical Sciences, State University of New York at Albany, NY, USA.

Running title: Complement evasion by CspZ in vertebrate hosts

Key words: Lyme disease, CspZ, *Borrelia*, Factor H, Complement

[†]Current address: Department of Biology, St. Mary's College of Maryland, St. Mary's, MD

*correspondence: Yi-Pin Lin, Ph.D.
Division of Infectious Diseases,
Wadsworth Center, New York State Department of Health
120 New Scotland Ave, Albany, NY 12208
Telephone: 518-402-2233; Fax: 518-473-1326
Email: Yi-Pin.Lin@health.ny.gov

SUMMARY (196 words)

Lyme disease, caused by the spirochete *Borrelia burgdorferi*, is the most common vector-borne disease in the US and Europe. The spirochetes are transmitted from mammalian and avian reservoir hosts to humans via ticks. Following tick bites, spirochetes colonize the host skin and then disseminate hematogenously to various organs, a process that requires this pathogen to evade host complement, an innate immune defense system. CspZ, a spirochete surface protein facilitates resistance to complement-mediated killing *in vitro* by binding to the complement regulator, factor H (FH). Low expression levels of CspZ in spirochetes cultivated *in vitro* or during initiation of infection *in vivo* has been a major hurdle in delineating the role of this protein in pathogenesis. Here we show that treatment of *B. burgdorferi* with human blood induces CspZ production and enhances resistance to complement. By contrast, a *cspZ*-deficient mutant and a strain that expressed a FH-nonbinding CspZ variant were impaired in their ability to cause bacteremia and colonize tissues of mice or quail; virulence of these mutants was however restored in complement C3-deficient mice. These novel findings suggest that FH-binding to CspZ facilitates *B. burgdorferi* complement evasion *in vivo* and promotes systemic infection in vertebrate hosts.

INTRODUCTION

Lyme disease (LD) is the most common vector-borne illness in North America and Europe, with an estimated 300,000 new human cases occurring annually in the US (Hinckley et al., 2014; Steere et al., 2016). In North America, LD is primarily caused by the spirochete *Borrelia burgdorferi* sensu stricto (hereafter *B. burgdorferi*), which is transmitted by *Ixodes* ticks and maintained in various vertebrate reservoir hosts (mainly mammals and birds) (Brisson,

45 Drecktrah, Eggers, & Samuels, 2012; Eisen & Eisen, 2018). Following tick bites, the spirochetes
46 spread from the skin of inoculation site to multiple tissues and organs via the bloodstream
47 (Steere et al., 2016). In humans, infection with Lyme borreliae can result in long lasting, and
48 debilitating symptoms including arthritis, carditis, and neuroborreliosis (Steere et al., 2016).
49 Thus, dissemination and systemic infection require spirochetes to survive in the bloodstream of
50 their different hosts (Radolf, Caimano, Stevenson, & Hu, 2012).
51 Complement is one of the key host innate immune defense mechanisms (Meri, 2016;
52 Zipfel & Skerka, 2009). In general, complement can be activated on the surface of invading
53 pathogens by the classical, lectin, and/or alternative pathways. The classical pathway is initiated
54 on pathogens when antibodies bind to target antigens and engage the C1-complex. The lectin
55 pathway is activated when recognition molecules (mannan binding lectin (MBL), collectins or
56 ficolins) bind to select carbohydrates. The alternative pathway is initiated when activated C3b
57 binds to the pathogen surface. Activation of all three pathways leads to the formation of C3
58 convertases (C4b2a by the classical and lectin pathway, or C3bBb by the alternative pathway),
59 and further activation and deposition of C3b on C3 convertases lead to the formation of C5
60 convertases. These multi-protein complexes ultimately promote the release of proinflammatory
61 peptides, the deposition of opsonins (C3b and iC3b), and insertion of the pore-forming
62 membrane attack complex (MAC) (Merle, Church, Fremeaux-Bacchi, & Roumenina, 2015;
63 Merle, Noe, Halbwachs-Mecarelli, Fremeaux-Bacchi, & Roumenina, 2015; Zipfel & Skerka,
64 2009). Complement regulators such as Factor H (FH) and FH-like protein 1 (FHL-1, the
65 alternatively spliced form of FH) that bind to C3b to promote its degradation into iC3b (Sjoberg,
66 Trouw, & Blom, 2009; Zipfel & Skerka, 2009) and prevent excessive complement activation and
67 host cell damage in the absence of pathogens or tissue injury.

Pathogens have developed multiple mechanisms to escape killing by complement (Lambris, Ricklin, & Geisbrecht, 2008). One such mechanism is the production of complement-binding proteins to block the formation of complement complexes (Blom, Hallstrom, & Riesbeck, 2009; Kraiczy, 2016a; A. Marcinkiewicz, Kraiczy, & Lin, 2017; Meri, 2016). Another mechanism is to express complement regulator-binding proteins, which recruit host complement regulators to the cell surface to degrade active complement complexes (Blom et al., 2009; Meri, 2016). For example, Lyme borreliae produce OspC and BBK32, which respectively bind C4b and C1q to inhibit complement (Caine et al., 2017; Garcia, Zhi, Wager, Hook, & Skare, 2016). This pathogen also produces at least five distinct complement regulator-acquiring surface proteins (CRASPs): CspA (CRASP-1), CspZ (CRASP-2), ErpP (CRASP-3), ErpC (CRASP-4), ErpA (CRASP-5) (Kraiczy & Stevenson, 2013). These proteins bind to FH and/or FHL-1 (CspA and CspZ only) to inhibit the alternative pathway (Kraiczy & Stevenson, 2013). One of these FH-binding CRASPs, CspZ, promotes survival of otherwise serum-sensitive, non-pathogenic Lyme borreliae in human serum when overexpressed in these strains (Hartmann et al., 2006; Siegel et al., 2008). This protein is produced during mouse infection but not when the spirochetes reside in unfed or feeding ticks (Bykowski et al., 2007), suggesting a role of CspZ in providing bacteria the ability to survive in the hosts. However, a *cspZ*-deficient strain is fully infectious via needle infection (Coleman et al., 2008). Additionally, when mice were subcutaneously inoculated with a library of *B. burgdorferi* mutants carrying transposon insertions, mutants with transposon insertions in *cspZ* displayed only minor defects in colonization of mice (T. Lin et al., 2012). Interestingly, *B. burgdorferi* produces extremely low levels of CspZ when cultivated *in vitro* (Bykowski et al., 2007). This finding raises a possibility that low production of CspZ in *in*

vitro-cultivated wild type *B. burgdorferi* does not permit elucidation of differences in serum survival or infectivity between the wild type and the *cspZ*-deficient mutant strain.

Spirochetes produce distinct protein profiles when cultivated in different conditions *in vitro* or while infecting vertebrate animals (Brooks, Hefty, Jolliff, & Akins, 2003; Hyde, Trzeciakowski, & Skare, 2007; Ojaimi et al., 2003; Revel, Talaat, & Norgard, 2002; Seshu, Boylan, Gherardini, & Skare, 2004; Tokarz, Anderton, Katona, & Benach, 2004). Incubating *B. burgdorferi* with mammalian blood simulates the conditions in hosts that leads to upregulation of genes that are normally expressed when spirochetes are in vertebrate hosts (Tokarz et al., 2004). In fact, blood treatment of spirochetes has been used to delineate the roles of several spirochete genes *in vivo* (Caine & Coburn, 2015; Caine et al., 2017; Y. P. Lin et al., 2015; Moriarty et al., 2012; Norman et al., 2008). Therefore, we hypothesized that blood treatment of spirochetes would enhance the production of CspZ thereby permitting examination of this protein in facilitating serum survival and infectivity in diverse hosts. In this study, we tested this hypothesis and elucidated a novel role for CspZ-FH interactions in bacterial pathogenesis *in vivo*.

RESULTS

Treating *B. burgdorferi* with human blood enhances CspZ production. To define CspZ's role *in vitro* and *in vivo*, we obtained wild type (WT) infectious *B. burgdorferi* B31-A3 and its isogenic *cspZ*-deficient mutant, B31-A3Δ*cspZ* (Coleman et al., 2008). This mutant strain carrying shuttle vector pKFSS (B31-A3Δ*cspZ*-V) or complemented with a plasmid encoding WT *cspZ* were generated. We also constructed a shuttle vector encoding this gene's promoter from *B. burgdorferi* strain B31-A3 to drive *cspZ-Y207A/Y211A*, which produces the point mutant of CspZ defective in FH-binding activity (Siegel et al., 2008). This plasmid was transformed into

B31-A3Δ*cspZ* as to generate complemented strain as a negative control. Note that CspZ-Y207A/Y211A was chosen to specifically eliminate FH binding; a previous study showed that CspZ-Y207A/Y211A binds neither to human nor mouse FH (A. L. Marcinkiewicz et al., 2018; Siegel et al., 2008). This is because a hydrogen bond between FH and tyrosine-207 of CspZ is abolished in this mutant protein (PDB#6ATG, http://www.rcsb.org/structure/6ATG). We also found that CspZ-Y207A/Y211A does not bind to FH from *Coturnix* quail, the avian model of LD (Isogai et al., 1994), whereas WT CspZ bound (Fig. S1 bottom and Table 1). Further, recombinant CspZ-Y207A/Y211A protein maintained its secondary structure, similar to the recombinant CspZ, (Fig. S2) and displayed similar levels of fibronectin, laminin, and plasminogen binding as WT CspZ (Hallstrom et al., 2010) (Fig. S3 and Table S1).

Hypothesizing that CspZ production is upregulated by vertebrate animals' blood that simulates the host conditions, we first treated WT *B. burgdorferi* strain B31-A3 with human blood, and *cspZ* expression was quantitated by RT-PCR (qRT-PCR). Mid-log phase B31-A3 were incubated with that blood for 48 hours as previously described (Tokarz et al., 2004). We found that untreated and blood-treated spirochetes expressed similar levels of *recA*, a constitutively expressed gene (Fig. 1A). Untreated *B. burgdorferi* expressed low but detectable of *cspZ*, consistent with previous reports (Coleman et al., 2008; Hartmann et al., 2006; Rogers, Abdunnur, McDowell, & Marconi, 2009) (Fig. 1A). Blood-treated *B. burgdorferi* expressed 4.1-fold greater levels of *cspZ* compared to untreated spirochetes (Fig. 1A). We then sought to determine if increased *cspZ* expression translates to greater amounts of CspZ on the spirochete surface using flow cytometry (Fig. 1B). The periplasmic flagellin protein FlaB and the FH-binding protein CspA were used as controls. As expected, the production of FlaB was detectable in methanol-permeabilized but not in unpermeablized *B. burgdorferi* cells, consistent with the

periplasmic location of this protein (Kumru, Schulze, Slusser, & Zuckert, 2010; Limberger, 2004) (Fig. 1C). The levels of FlaB were indistinguishable between untreated and blood-treated cells (Fig. 1C). The production of CspA was indistinguishable between permeabilized and unpermeabilized cells, in agreement with CspA's surface localization (Fig. 1C) (Kraiczy et al., 2004). Consistent to previous work (Brooks et al., 2003; Bykowski et al., 2007; Tokarz et al., 2004), CspA levels decreased 3.3-fold in blood-treated compared to untreated cells (Fig. 1C). Finally, similar levels of CspZ was detected on permeabilized and unpermeablized strain B31-A3 (Fig. 1C), in agreement with this protein localized on the surface (Bykowski et al., 2007; Dowdell et al., 2017; Hartmann et al., 2006). Strikingly, the 5.3-fold enhancement of CspZ production in the presence of human blood compared to untreated strain B31-A3 (Fig. 1B and C). Further, we incubated blood with B31-A3Δ*cspZ*-V or B31-A3Δ*cspZ* producing WT *cspZ* or *cspZ-Y207A/Y211A*. Similarly, the strain B31-A3Δ*cspZ* producing WT *cspZ* or *cspZ-Y207A/Y211A* exhibited enhanced CspZ production whereas these strains and the B31-A3Δ*cspZ*-V displayed decreased CspA production after blood treatment (Fig. 1D to F). Note that all these strains displayed indistinguishable levels of viability and generation time in either untreated or blood treated conditions. These results suggest that spirochete growth is not altered, and there is no difference among strains regarding to viability after blood treatment (Fig. S4 and Table S2 and S3). Taken together, these findings indicate that blood treatment induces CspZ production and down-regulates CspA production in the *B. burgdorferi* strains that encode the genes to produce these proteins.

CspZ requires Tyrosine-207 and -211 to promote blood-treated *B. burgdorferi* binding to human, mouse, and quail FH. To define the role of CspZ in binding to human, mouse, and

quail FH when expressed on the spirochete surface, FH purified from these hosts were incubated with *in vitro* cultivated, untreated (no added blood) B31-A3, B31-A3Δ*cspZ*-V, and bacteria-bound FH was detected by flow cytometry. A high passage and non-infectious *B. burgdorferi* strain B313 was also included as a negative control because this strain lacks the plasmids encoding CspZ and CspA (Hallstrom et al., 2013). We found that the level of these hosts' FH bound by B31-A3 and B31-A3Δ*cspZ*-V were greater than that by B313 but undistinguishable between each other (Fig. S5). These findings indicated that in the absence of blood treatment, FH binding to B31-A3 and B31-A3Δ*cspZ*-V were similar. To enhance CspZ production in the wild-type isolate and downregulate CspA production in both wild-type and mutant, we treated these strains with human blood and assessed binding of human, mouse, and quail FH to each of these spirochete strains. As expected, B313 bound nearly undetectable levels of these hosts' FH (Fig. 2) (Hart, Nguyen, et al., 2018; Hartmann et al., 2006). Consistent with previous observations (Hart, Nguyen, et al., 2018; Kenedy, Vuppala, Siegel, Kraiczy, & Akins, 2009; McDowell et al., 2003), B31-A3 bound FH from all three species (Fig. 2). Although B31-A3Δ*cspZ*-V still retained the ability to bind to these hosts' FH, possibly due to the production of other FH-binding proteins, this CspZ-deficient strain showed over 4-fold reduced levels of FH binding compared to B31-A3 (Fig. 2). These findings indicate that prior blood treatment of spirochetes is necessary to reveal binding of FH to CspZ. We also treated blood with B31-A3Δ*cspZ* producing WT CspZ or CspZ-Y207A/Y211A and determine their ability to bind to human, mouse or quail FH. Ectopically produced CspZ but not CspZ-Y207A/Y211A in B31-A3Δ*cspZ*-V restored binding to these hosts' FH (Fig. 2). The *cspZ-Y207A/Y211A*-complemented strain bound to these FH molecules 4-fold less than the *cspZ*-complemented strain (Fig. 2). These findings indicate that

tyrosines at positions 207 and 211 of CspZ are required for maximal binding of human, mouse, and quail FH.

CspZ-mediated FH-binding contributes to reduced MAC deposition on the surface of blood-treated spirochetes. Next, we asked if the FH-binding activity of CspZ reduced the deposition of complement activation products on the spirochete surface. We incubated WT strain B31-A3, B31-A3Δ*cspZ*-V, and B313 with 20% of human or mouse serum and quantified the levels of MAC bound to the spirochete surface using flow cytometry (Fig. 3). Quail serum could not be assessed due to the unavailability of antibodies that recognize avian MAC. The levels of MAC deposited on the surface of WT strain B31-A3 and B31-A3Δ*cspZ*-V were similar, but lower than that on the strain B313 (Fig. S6A and B). To enhance the production of CspZ, we treated these strains with human blood prior to incubation with serum to measure the levels of surface-associated MAC. As expected, a significant amount of human and mouse MAC could be detected on B313 whereas MAC deposition on the WT strain B31-A3 was undetectable (Fig. 3). Strain B31-A3Δ*cspZ*-V deposited greater amounts of MAC compared to the WT strain B31-A3 but lower levels compared to strain B313 (Fig. 3B). We also treated B31-A3Δ*cspZ* complemented with *cspZ* or *cspZ Y207A/Y211A* with human blood prior to incubating them with serum. MAC deposition was undetectable on the surface of the strain complemented with the WT *cspZ* gene as expected (Fig. 3B) while significant amounts of human and mouse MAC were deposited on the strain complemented with the *cspZ-Y207A/Y211A* (Fig. 3B). These results indicate that blood treatment of spirochetes, which enhances CspZ expression and FH binding, translates to inhibition of human and non-human complement deposition.

CspZ binding to FH facilitates blood-treated *B. burgdorferi* to survive in serum. We aimed to determine CspZ's role in promoting spirochete survival in serum. The WT strain B31-A3 and B31-A3Δ*cspZ*-V were incubated with human or quail serum, or negative control sera that were not expected to kill bacteria (C3-depleted human serum or heat inactivated human or quail serum) for four hours. Mouse serum was not tested because mouse complement is highly unstable *ex vivo* (Caine & Coburn, 2015; Lachmann, 2010; A. Marcinkiewicz et al., 2017; Ristow et al., 2012). Consistent with previous findings (Coleman et al., 2008), we found that nearly 100% of the WT strain B31-A3 and B31-A3Δ*cspZ*-V survive in human, quail, and negative control sera (Fig. S7). We then treated the WT strain B31-A3 or B31-A3Δ*cspZ*-V with human blood to enhance expression of *cspZ* prior to incubation with sera. Over 75% of the WT strain B31-A3 survived in active (Fig. 4 top panel) or C3-depleted human serum (Fig. 4 middle panel). While less than 50% of the strain B31-A3Δ*cspZ*-V were viable in human serum (Fig. 4 top panel), this strain survived almost 100% in heat-inactivated (Fig. 4 top panel) or C3-depleted human serum (Fig. 4 middle panel). Similarly, approximately 100% of WT strain B31-A3 survived in quail serum (Fig. 4 bottom panel). Although only 36% of B31-A3Δ*cspZ*-V remained motile in this serum, it showed nearly 100% survival in heat-inactivated quail serum (Fig. 4 bottom panel). These findings indicate that CspZ promotes blood-treated spirochetes to survive in human and quail sera.

The serum resistance of B31-A3Δ*cspZ*-V complemented with *cspZ* or *cspZ-Y207A/Y211A* was also assessed using identical experimental conditions. Approximately 75% of the *cspZ*-complemented strain survived in both active or C3-depleted human serum (Fig. 4 top and middle panel). Only 25% of the *cspZ-Y207A/Y211A*-complemented strain survived in human serum (Fig. 4 top panel) but retained close to 100% viability in heat-inactivated (Fig. 4 top panel) or C3-

depleted human serum (Fig. 4 middle panel). Almost 100% of the *cspZ*-complemented bacteria survived in quail serum while only 36% of the *cspZ-Y207A/Y211A*-complemented strain was viable (Fig. 4 bottom panel). Moreover, almost 100% of bacteria of this strain remained motile in heat-inactivated quail serum (Fig. 4 bottom panel). These results suggest that CspZ-mediated FH-binding activity provides serum resistance activity for blood-treated *B. burgdorferi*.

FH binding to CspZ confers bacteremia and tissue colonization of blood-treated *B. burgdorferi*. We next asked whether CspZ-mediated FH-binding promotes infectivity in mice. Subcutaneous needle infection of spirochetes with the dose close to ID_{50} (the dose that infects 50% of animals) often reveals subtle *in vivo* phenotypes conferred by spirochete genes that are expressed in hosts (Blevins, Hagman, & Norgard, 2008; Hyde et al., 2011; Seshu et al., 2006; Shi, Xu, Seemanaplli, McShan, & Liang, 2008; Weening et al., 2008). We thus introduced 10^3 cells of WT strain B31-A3 or B31-A3Δ*cspZ*-V into BALB/c mice (the ID_{50} of strain B31-A3 is ~10^3 cells (Showman, Aranjuez, Adams, & Jewett, 2016; Tilly et al., 2006)). We then used quantitative PCR (qPCR) to quantify spirochete burdens in the bloodstream and tissues. The infection of WT strain B31-A3 or strain B31-A3Δ*cspZ*-V resulted in indistinguishable levels of bacteremia at 7 days post-infection (dpi) and tissue colonization at both 7 and 14 dpi (Fig. S8A left panel and 8B to E). Note that we were unable to detect spirochetes in the blood at 14 dpi (Fig. S8A right panel), in agreement with kinetics of bacteremia present only at extremely early stages of murine infection (Caine et al., 2017).

In order to delineate the role of CspZ during the course of infection, we treated WT strain B31-A3 and B31-A3Δ*cspZ*-V with human blood to upregulate *cspZ* expression. BALB/c mice were then infected with blood-treated B31-A3 or B31-A3Δ*cspZ*-V. Bacteremia triggered by the

former strain was observed at 7 dpi but not at 14 dpi (Fig. 5A). Colonization was detected for WT strain B31-A3 in all tested tissues at 7 and 14 dpi (Fig. 5B to E). In contrast, the strain B31-A3Δ*cspZ*-V induced six-fold less levels of bacteremia at 7 dpi ($p = 0.021$, Fig. 5A left panel) and displayed 2600 and 9-fold lower spirochete burden at the inoculation site than the WT strain at 7 and 14 dpi, respectively ($p < 0.05$, Fig. 5B). The *cspZ*-deficient strain also exhibited a lower, although not statistically significant, level of colonization of the heart, bladder, and joints compared to the WT strain at 7dpi (Fig. 5C to E left panel). At 14 dpi, the *cspZ*-deficient mutant colonized these tissues at 6- to 9-fold reduced levels compared to the WT strain (Fig. 5 C to E right panel). We also infected mice with human blood-treated B31-A3Δ*cspZ* producing WT CspZ or CspZ-Y207A/Y211A. Ectopically producing WT CspZ but not CspZ-Y207A/Y211A in the strain B31-A3Δ*cspZ* restores the defect of bloodstream survival at 7 dpi (5-fold greater bacterial burdens than the strain B31-A3Δ*cspZ*-V, Fig. 5A left panel). At 7 and 14dpi, the *cspZ-Y207A/Y211A*-complemented strain did not colonize the inoculation site while the *cspZ*-complemented strain did (13 to 259-fold greater levels than the strain B31-A3Δ*cspZ*-V) (Fig. 5B). These strains did not display different levels of colonization in heart, bladder, and joints at 7dpi (Fig. 5C to E left panel). However, at 14 dpi, the *cspZ*-complement strain exhibited 2.4 to 13-fold greater levels of colonization at these tissues compared to B31-A3Δ*cspZ*-V. Spirochetes producing CspZ-Y207A/Y211A colonized these tissues with a bacterial burden similar to the strain B31-A3Δ*cspZ*-V (Fig. 5C to E right panel). These results demonstrate that CspZ-mediated FH-binding promotes hematogenous dissemination of blood-treated spirochetes in mice.

Complement evasion mediated by CspZ-FH interactions facilitates blood-treated spirochete to survive in mouse bloodstream and tissues. We next sought to investigate

whether CspZ-mediated FH-binding activity, by evading the complement, facilitates blood-treated spirochetes to survive in mouse bloodstream and tissues. We first subcutaneously inoculated C3-deficient mice in a BALB/c background ($C3^{-/-}$ mice) with 10^3 cells of each of the four following spirochete strains after treating these strains with human blood. These strains include WT strain B31-A3, B31-A3Δ*cspZ*-V, B31-A3Δ*cspZ* complemented with *cspZ*, or *cspZ Y207A/Y211A* mutant. qPCR was used to measure spirochete loads in the bloodstream and tissues. In contrast to the findings in WT mice, we found no differences in bacterial burdens across all four strains in bloodstream at 7 dpi (Fig. 6A) and the inoculation site, heart, bladder, and joints of $C3^{-/-}$ mice at 7 and 14 dpi (Fig. 6B to E). These results indicate that that FH binding to CspZ facilitates blood-treated *B. burgdorferi* to evade mouse complement and thus renders them pathogenic.

FH binding activity of CspZ promotes spirochete colonization in quail. We aimed to test whether CspZ-mediated FH-binding confers infectivity of *B. burgdorferi* in avian hosts such as the quail. We thus treated WT strain B31-A3 with human blood to enhance the production of CspZ, subcutaneously inoculated 10^6 cells of B31-A3 cells into quail, and determined bacterial burdens using qPCR in the blood and tissues. We could not detect WT strain B31-A3 in the blood or any tested tissues at 3 dpi (detection limit: one bacterium per one microgram of DNA, Fig. S9). Although we were still unable to detect spirochetes in the blood, live or heart at 7 dpi, spirochetes were detectable at the inoculation site and the brain at this time point (Fig. 7 and S9). The viability of spirochetes in these tissues was verified microscopically after culturing the tissues collected from the quail at 7 dpi: five out of six quail inoculation sites and brain tissues were culture positive. We also subcutaneously infected quail with human blood-treated B31-

A3Δ*cspZ*-V, or this strain producing CspZ or CspZ-Y207A/Y211A. At 7 dpi, the strain B31-A3Δ*cspZ*-V colonized the inoculation site and brain approximately five to eight-fold less, respectively, compared to WT strain B31-A3 (Fig. 7). Ectopically producing CspZ in B31-A3Δ*cspZ* restored the colonization defects in these tissues (Fig. 7), indicating CspZ contributes to *B. burgdorferi* colonization at quail tissues. However, ectopic production of CspZ-Y207A/Y211A did not restore colonization levels in the inoculation site and brain (similar spirochete burdens to mutant B31-A3Δ*cspZ*-V) (Fig. 7). These results suggest that CspZ binds to FH to facilitate spirochetes to establish infection and promote dissemination in quail.

DISCUSSION

B. burgdorferi, the causative agent of LD, produces at least 86 outer surface lipoproteins (Dowdell et al., 2017). Although some of these proteins are produced in abundance, most are expressed at low levels when cultured *in vitro* and/or during murine infection (Kenedy, Lenhart, & Akins, 2012), which have been hurdles in studying their roles in pathogenesis. Cultivating *B. burgdorferi* in specific conditions such as blood supplemented growth media to induce the production of proteins of interest has been utilized to investigate the role of such proteins *in vitro* and *in vivo* (Kumar et al., 2015; Moriarty et al., 2012; Parveen & Leong, 2000; Zhi et al., 2015). We used human blood to treat spirochetes and observed induction of CspZ (Fig. 1) as this host's blood has been used as a host-simulated cue to alter the expression of spirochetes genes (Tokarz et al., 2004). However, the varying molecular compositions of the blood of different animal species (Hamdy, 1977; Sojka et al., 2013; Wickramasekara, Bunikis, Wysocki, & Barbour, 2008), raising the possibility that enhanced *cspZ* expression is host blood-specific, which warrants further investigation. Additionally, human blood treatment of spirochetes followed by murine

infection may not reflect to the nature life cycle of Lyme borreliae in mice. This concern could be eased by treating spirochetes with mouse blood prior to infection for future studies. Further, Tokarz et al. did not report an increased *cspZ* expression in spirochetes treated with human blood using a microarray, which could be due to the stringent criteria used to define the differential gene expression (Tokarz et al., 2004). Treating *B. burgdorferi* with proteases has been commonly used to determine a particular spirochete protein's surface localization (El-Hage et al., 2001; Exner, Wu, Blanco, Miller, & Lovett, 2000; Zuckert, Kerentseva, Lawson, & Barbour, 2001). CspZ remains intact after the treatment of proteinase K and trypsin, suggesting this protein's resistance to digestion by these proteases (Coleman et al., 2008; Dowdell et al., 2017; Hartmann et al., 2006). However, CspZ is eliminated when spirochetes are treated with pronase (Dowdell et al., 2017), a protease isolated from *Streptomyces griseus* (Hiramatsu & Ouchi, 1963). This finding indicates this protein's surface localization, consistent with our and previous observations using fluorescence-based methodologies (Bykowski et al., 2007; Hartmann et al., 2006; Siegel et al., 2008)(Fig. 1B, C, E, and F).

We found that blood treatment is essential to demonstrate the CspZ-mediated FH-binding activity to confer spirochete survival in sera (Fig. 4). It is noteworthy that we count immotile cells as the indicator of cell death by dark-field microscopy, a method which has been commonly used to identify killed cells (Alitalo et al., 2005; Alitalo et al., 2001; Brooks et al., 2005; Kraiczy, Hunfeld, Peters, et al., 2000; McDowell et al., 2011; van Dam et al., 1997). Furthermore, the lack of motility is the most apparent sign of complement-mediated bacterial killing, which allows determination of cell viability microscopically without the need for the extended duration of time to cultivate spirochetes. Further, the ability of pathogens to limit complement activation on their surface often correlates with their ability to survive in the

342 bloodstream and cause systemic infection (Lambris et al., 2008; Roantree & Rantz, 1960). For
343 example, the *B. burgdorferi* outer surface protein BBK32 inhibits activation of the classical
344 pathway and confers resistance to human serum (Garcia et al., 2016). This protein also promotes
345 spirochete survival in the mouse bloodstream and dissemination (Caine & Coburn, 2015; Hyde et
346 al., 2011; Seshu et al., 2006). Similarly, *B. burgdorferi* produces OspC that inactivates both
347 classical and lectin pathways and contributes to early stages of bacteremia (Caine & Coburn,
348 2015; Caine et al., 2017). In this study, we treated a *cspZ*-deficient *B. burgdorferi* with blood to
349 demonstrate this CspZ's ability, by evading complement, to promote bacteremia and/or tissue
350 colonization (Fig. 5 and 6). Note that this finding does not imply that CspZ facilitates spirochete
351 survival in fed ticks during transmission as *B. burgdorferi* does not produce CspZ when it is in
352 either post molting flat nymphs or feeding nymphs (Bykowski et al. Infect Immun. 2007).
353 However, CspZ is produced at low levels in the biting site of skin after transmission (Bykowski
354 et al. Infect Immun. 2007). Therefore, in the case that a *cspZ*-deficient spirochete displays defect
355 of infectivity in vertebrate hosts during transmission, CspZ's role should be dependent on the
356 host environment such as skin. Further, *B. burgdorferi* has been shown to more efficiently spread
357 to distal tissues in mice deficient of some complement proteins (e.g. $C3^{-/-}$ or $C1q\alpha^{-/-}$ mice)
358 Compared to WT mice (Lawrenz et al., 2003; Woodman et al., 2007; Zhi, Xie, & Skare, 2018).
359 Similarly, we observed increased spirochete burdens in the tissues of $C3^{-/-}$ mice (Fig. 6B to E)
360 relative to the WT mice (Fig. 6B to D) at 14dpi, suggesting the need for *B. burgdorferi* to evade
361 complement in order to disseminate. Further, the initial skin colonization of *B. burgdorferi*
362 results in an exuberant inflammatory response at inoculation site of dermis (Antonara, Ristow,
363 McCarthy, & Coburn, 2010; Hovius et al., 2009; Xu, Seemanapalli, Reif, Brown, & Liang,
364 2007). Complement in the vascular compartment or interstitial fluid would accompany the

365 localized influx of cells at the dermal inoculation site (Wilhelm, 1973). This addresses our
366 finding that spirochetes use the FH-binding activity of CspZ to establish infection at inoculation
367 site (Fig. 5B and 6B).

368 In addition to mammals, birds also maintain Lyme borreliae as a reservoir host in the
369 enzootic cycle (Brisson et al., 2012; Eisen & Eisen, 2018). However, the molecular mechanisms
370 of spirochete colonization and dissemination in this host remain unclear. This could be due to the
371 cumbersome work of maintaining wild-caught birds and/or the inability to persistently infect
372 some avian hosts with Lyme borreliae experimentally (Bishop, Khan, & Nielsen, 1994; Burgess,
373 1989; Ginsberg et al., 2005; Isogai et al., 1994; Kurtenbach et al., 1998; Kurtenbach, Schafer, et
374 al., 2002; Olsen, Gylfe, & Bergstrom, 1996; Piesman, Dolan, Schriefer, & Burkot, 1996; Richter,
375 Spielman, Komar, & Matuschka, 2000). Among these avian species, *Coturnix* quail is capable of
376 harboring Lyme borreliae for at least eight weeks after needle infection (Isogai et al., 1994).
377 Similar to previous findings (Isogai et al., 1994), we did not detect spirochetes in the blood
378 during infection (Fig. S9), reiterating the inability of Lyme borreliae to induce high levels of
379 bacteremia in vertebrate animals (Steere et al., 2016). Unlike a previous study detecting
380 spirochetes in the liver and heart of *B. garinii*-infected quail (Isogai et al., 1994), we did not
381 observe *B. burgdorferi* colonization at these sites, possibly reflecting strain-specific tissue
382 tropism (Fig. S9)(Craig-Mylius, Lee, Jones, & Glickstein, 2009; Jones et al., 2006; Wang, van
383 Dam, Schwartz, & Dankert, 1999). We found that CspZ-mediated FH-binding activity facilitates
384 spirochete colonization at the quail inoculation site and brain, which reveals the role of a B.
385 *burgdorferi* protein in promoting avian host competence at the first time (Fig. 7). Note that Not
386 every strain of Lyme borreliae species encodes CspZ (Kingry et al., 2016; Kraiczy, Skerka,
387 Brade, & Zipfel, 2001; Rogers & Marconi, 2007), and allelic variations confer differential

388 human FH/FHL-1-binding activity (Kraiczy et al., 2008; Kraiczy et al., 2001; Rogers et al.,
389 2009). This raises the possibility that CspZ variants may determine host-specificity of FH-
390 binding and determine the animals' competence to each strain (Bhide et al., 2005 ; Kraiczy,
391 2016b; Kurtenbach, De Michelis, et al., 2002). This could be further investigated using the quail
392 and mouse as Lyme infection models established in this study. Such models can also be applied
393 to study the role of additional proteins of *B. burgdorferi* or other pathogens that are induced
394 during blood treatment in promoting infectivity. Gaining an understanding of the mechanisms of
395 pathogen infectivity can permit further efforts to find treatments or vaccines to improve human
396 health.
397
398 **EXPERIMENTAL PROCEDURES**
399 **Ethics statement.** All mouse experiments were performed in strict accordance with all
400 provisions of the Animal Welfare Act, the Guide for the Care and Use of Laboratory Animals,
401 and the PHS Policy on Humane Care and Use of Laboratory Animals. The protocol was
402 approved by the Institutional Animal Care and Use Committee (IACUC) of Wadsworth Center,
403 New York State Department of Health (protocol Docket Number 16-451), and University of
404 Massachusetts Medical School (protocol Docket Number 1930). All efforts were made to
405 minimize animal suffering.
406
407 **Mouse, quail, bacterial strains, and animal sera.** Swiss Webster mice used to generate anti-
408 serum against CspZ and BALB/c mice were purchased from Charles River (Wilmington, MA)
409 and Taconic (Hudson, NY), respectively. $C3^{-/-}$ mice (C57BL/6) purchased from Jackson
410 Laboratory (Bar Harbor, ME) were backcrossed for 11 generations into a BALB/c background.

Mice were genotyped for the C3 alleles by PCR analysis of mouse tail DNA (Table S4). *Coturnix coturnix* quail were purchased from Cavendish Game Bird Farm (Springfield, VT). The *Borrelia* and *Escherichia coli* strains used in this study are described in Table 2. All *B. burgdorferi* strains were grown at 33°C in BSK-II complete medium supplemented with kanamycin (200µg/mL), streptomycin (50µg/mL), or no antibiotics as required. For blood-treatment, spirochetes were incubated with human blood as described (Tokarz et al., 2004). Approximately 5 x 10^6 cells of mid-log *B. burgdorferi* were cultivated in BSK-II complete medium with 5% human blood with the buffy coat removed. This concentration of human blood does not reduce the growth and motility of serum-sensitive strains (Breitner-Ruddock, Wurzner, Schulze, & Brade, 1997; Hart, Nguyen, et al., 2018; Kenedy & Akins, 2011; van Dam et al., 1997). The human blood was supplemented with a cocktail of antibiotics (final concentration: 50µg/mL rifampicin, 20µg/mL phosphomycin and 2.5µg/mL amphotericin) to prevent potential bacterial and fungal contamination. Spirochetes were then incubated with human blood at 33°C at 2% CO_2 under a microaerophilic condition for 48 hours prior to use. *E. coli* strains were grown at 37°C in Luria-Bertani (BD Bioscience, Franklin Lakes, NJ) broth or agar, supplemented with kanamycin (50µg/mL), streptomycin (50 µg/mL), ampicillin (100µg/mL), or no antibiotics (Table 2). Human, mouse, and quail sera were obtained from and MB Biomedical, Inc (Santa Ana, CA), Southern Biotech, Inc (Birmingham, AL), and Canola Live Poultry Market (Brooklyn, NY), respectively. Prior to being used, these sera were screened with the C6 Lyme ELISA kit (Diamedix, Miami Lakes, FL) to determine whether the individual from which it was collected had prior exposure to *B. burgdorferi* by detecting antibodies against the C6 peptide of the *B. burgdorferi* protein VlsE (Lawrenz et al., 1999).

Generation of recombinant CspZ proteins and antisera. The open reading frames lacking the putative signal sequences of *bbh06* (*cspZ*) or encoding CspZ-Y207A/Y211A (CspZ with tyrosine-207 and -211 replaced by alanine residues) from *B. burgdorferi* strain B31-A3 was amplified using listed plasmids and primers (Table 2 and S4)(Siegel et al., 2008). Amplified fragments were engineered to encode a BamHI site at the 5' end and a stop codon followed by a SalI site at the 3' end. PCR products were sequentially digested with BamHI and SalI and then inserted into the BamHI and SalI sites of pGEX4T2 (GE Healthcare, Piscataway, NJ). The plasmids were sequenced and then transformed into *E. coli* strain BL21(DE3) (Wadsworth ATGC facility). The GST-tagged CspZ proteins were produced and purified by GST affinity chromatography according to the manufacturer's instructions (GE Healthcare, Piscataway, NJ). Antisera against CspZ were generated by immunizing four-week-old Swiss Webster mice with each of the CspZ proteins as described (Benoit, Fischer, Lin, Parveen, & Leong, 2011).

Quantitative RT-PCR and PCR. For quantitative RT-PCR (qRT-PCR), RNA was extracted from *B. burgdorferi* strain B31-A3 using Direct-Zol RNA MiniPrep Plus Kit (Zymo Research, Irvine, CA), and contaminating DNA was removed using RQ1 RNase-Free DNase (Promega, Madison, WI). cDNA was synthesized from 1 μg of RNA using qScript cDNA SuperMix (Quanta Bioscience, Beverly, MA). The quantification of *16s rRNA*, *cspZ*, or *rec*A expression from cDNA using listed primers Table S4 (Hodzic et al., 2013)(Bykowski et al., 2007)(Hodzic, Feng, & Barthold, 2013; Morrison, Ma, Weis, & Weis, 1999). For quantitative PCR (qPCR), DNA was extracted using EZ-10 Spin Column Blood DNA Mini-Prep Kit (BioBasic, Inc., Markham, Ontario, Canada). The quantity and quality of DNA for each tissue sample were assessed by measuring the concentration of DNA and the ratio of the UV absorption at 260 to

280 using a Nanodrop 1000 UV/Vis spectrophotometer (ThermoFisher, Waltham, MA). The 280:260 ratio was between 1.75 to 1.85, indicating the lack of contaminating RNA or proteins. qPCR was performed to quantify spirochete loads through amplification of the *recA* gene as described (Table S4)(Y. P. Lin et al., 2014). Both qRT-PCR and qPCR were performed using an Applied Biosystems 7500 Real-Time PCR system (ThermoFisher) in conjunction with PowerUp SYBR Green Master Mix (ThermoFisher). Cycling parameters were 50°C for 2 minutes, 95°C for 10 minutes, and 45 cycles of 95°C for 15 seconds, and 60°C for 1 minute. Each biological replicate was run in duplicate and checked for intra-run variation. For qPCR, the number of *recA* copies was calculated by establishing a threshold cycle (Cq) standard curve of a known number of the *recA* gene extracted from cultivated *B. burgdorferi* B31-A3. To assure low signals were not due to the presence of PCR inhibitors, five samples from the blood, tibiotarsal joint, and bladder of mice, or the inoculation site and brain of quail were used in qPCR using mouse nidogen primers or quail β-actin (Table S4)(Hart, Yang, Pal, & Lin, 2018; Y. P. Lin et al., 2014). As predicted, we detected 10^7 copies of the mouse nidogen or quail β-actin gene from 100ng of each DNA sample, ruling out the presence of PCR inhibitors in these samples. For qRT-PCR, the gene expression of *cspZ* or *recA* was normalized to that of *16s rRNA* using the ΔCq method, where the relative expression of the target (*cspZ* or *recA*), normalized to the expression of *16s rRNA*, is given by $2^{-\Delta Cq}$, where Cq is the cycle number of the detection threshold (Equation 1).

$$cspZ \text{ or } recA \text{ expression relative to } 16s\ rRNA = 2^{-(Cq(16s\ rRNA)-Cq(cspZ \text{ or } recA))} \quad \text{(Equation 1)}$$

Circular dichroism (CD) spectroscopy. CD analysis was performed on a Jasco 810 spectropolarimeter (Jasco Analytical Instrument, Easton, MD) under nitrogen. CD spectra were measured at room temperature (RT, 25°C) in a 1mm path length quartz cell. Spectra of 10μM

CspZ or CspZ-Y207A/Y211A were recorded in phosphate based saline buffer (PBS) at RT, and three far-UV CD spectra were recorded from 190 to 250nm in 1nm increments. The background spectrum of PBS without protein was subtracted from the protein spectra. CD spectra were initially analyzed by the software Spectra Manager Program (Jasco). Analysis of spectra to extrapolate secondary structures were performed by Dichroweb (http://www.cryst.bbk.ac.uk/cdweb/html/home) using the K2D and Selcon 3 analysis programs (Y. P. Lin et al., 2009).

ELISA assays. A ELISA for FH, fibronectin, plasminogen, and laminin binding by CspZ proteins was performed as described (Y. P. Lin et al., 2009). One microgram of BSA (negative control; Sigma-Aldrich, St. Louis, MO), quail FH previously purified from quail serum (Hart et al. PLoS Pathog. 2018), human FH (ComTech, Tyler, Texas), plasma fibronectin, plasma plasminogen, or mouse laminin (Sigma-Aldrich) was coated onto microtiter plate wells. One hundred microliters of increasing concentrations (0.03125, 0.0625, 0.125, 0.25, 0.5, 1, 2μM) of GST (negative control) or GST-tagged CspZ or CspZ-Y207A/Y211A was then added to the wells. Mouse anti-GST tag (ThermoFisher; 1:200x) and HRP-conjugated goat anti-mouse IgG (ThermoFisher; 1:1,000x) were used as primary and secondary antibodies, respectively, to detect the binding of GST-tagged proteins. The plates were washed three times with PBST (0.05% Tween 20 in PBS), and 100μL of tetramethyl benzidine solution (ThermoFisher) was added to each well and incubated for five minutes. The reaction was stopped by adding 100μL of 0.5% hydrosulfuric acid to each well. Plates were read at 405nm using a Tecan Sunrise Microplate reader (Tecan, Morrisville NC). To determine the dissociation constant (K_D), the data were fitted with Equation 2 using GraphPad Prism software (GraphPad, La Jolla, CA).

503 $$OD405 = \frac{OD405max[CspZ\ proteins]}{KD+[CspZ\ proteis]}$$ (Equation 2)

504

505 **Shuttle vector construction and plasmid transformation into *B. burgdorferi*.** *cspZ* or *cspZ-*
506 *Y207A/Y211A* was first PCR amplified with the addition of a SalI site and a BamH1 site at the
507 5'and 3' ends, respectively, using Taq DNA polymerase (Qiagen) and primers listed in Table S4.
508 The unpaired nucleotides at 5' and 3' end of the amplified DNA fragments were removed with
509 an exonuclease from CloneJet PCR cloning kit (ThermoFisher) and then inserted into the vector
510 pJET1.2/blunt (ThermoFisher). The plasmids were then digested with SalI and BamHI to release
511 *cspZ* and *cspZ-Y207A/Y211A*, which were then inserted into the SalI and BamHI sites of pKFSS-
512 1 (Frank, Bundle, Kresge, Eggers, & Samuels, 2003)(Table 2). The promoter region of *cspZ*
513 from *B. burgdorferi* B31, 125bp upstream from the start codon of *cspZ*, was also PCR amplified
514 (Hartmann et al., 2006), added with SphI and SalI sites at the 5'and 3' ends, respectively, using
515 primers listed in Table S4. Promoter fragments were then inserted into the SphI and SalI sites of
516 pKFSS-1 to drive the expression of *cspZ* and *cspZ-Y207A/Y211A*. Electrocompetent *B.*
517 *burgdorferi* B31-A3Δ*cspZ* prepared as described (Samuels, 1995) was then transformed
518 separately with at least 44μg of each of the shuttle plasmids (Table 2) and cultured in BSK-II
519 medium at 33ºC for 24 hours. Liquid plating transformations were performed in the presence of
520 antibiotic selection (kanamycin and/or streptomycin) as described (Moriarty et al., 2012; Yang,
521 Pal, Alani, Fikrig, & Norgard, 2004). PCR and Sanger sequencing of resulting spirochete strains
522 were performed with primers specific for *colE1* and *cspZ*, respectively, to verify the presence of
523 pKFSS-1 and the insert in the transformants (Table S4). The plasmid profiles of these
524 spirochetes were examined as described (Purser & Norris, 2000) to ascertain identical profiles
525 between these strains and their parental strain B31-A3.

Determination of the viability and generation time of spirochetes. To determine spirochete viability after blood treatment, *B. burgdorferi* strains were cultivated in triplicate in untreated or human blood-treated conditions. After resuspending spirochetes in BSK-II medium without rabbit serum, they were stained for 15 minutes with 1x SYBR Green I (ThermoFisher) and 6µM propidium iodide (ThermoFisher) in 0.5% BSA in PBS as described (Feng, Wang, Zhang, Shi, & Zhang, 2014). The live (green) and dead (red) spirochetes were then visualized under overlaid FITC and Texas Red filters using Olympus BX51 fluorescence microscopy (Olympus Corporation, Waltham, MA). An image of four fields of view were taken to determine the proportion of live to dead spirochetes. Additionally, after growing for 48 hours with or without human blood, each of these strains (10^6 spirochetes/mL) was cultivated BSK II medium without human blood in triplicate to determine the spirochetes' generation time. The concentration of the spirochetes was calculated microscopically in triplicate every 24 hours. We then calculated the generation time for each strain in exponential phase (G) as previously described (Heroldova, Nemec, & Hubalek, 1998).

Flow cytometry. CspZ production, FH binding, and MAC deposition on spirochete surface were determined as described (Hart, Nguyen, et al., 2018). To evaluate the surface localization of CspZ, the spirochetes (1 x 10^8 cells) were washed with HBSC buffer containing glucose and BSA (HBSC-DB, 25mM Hepes acid, 150mM sodium chloride, 1mM $MnCl_2$, 1mM $MgCl_2$, 0.25mM $CaCl_2$, 0.1% glucose, and 0.2% BSA) and then resuspended into the same buffer. To permeabilize spirochetes, they were incubated with 100% methanol for an hour, followed by washed with HBSC-DB. Mouse antiserum raised against CspZ or CspA, or mouse anti-FlaB

monoclonal antibody was used as the primary antibody (1:250x). An Alexa 647-conjugated goat anti-mouse IgG (ThermoFisher) (1:250x) was used as the secondary antibody. To determine the ability of these *B. burgdorferi* strains to bind to FH, spirochetes (1 x 10^8 cells) were suspended in PBS and then incubated with 1 μg of human, mouse, or quail FH at 25ºC for one hour. The spirochetes were then washed with PBS and resuspended in HBSC-DB. A sheep anti-FH polyclonal IgG (ThermoFisher) (1:250x) or a mouse anti-FH monoclonal antibody VIG8 (1:250x) was used as the primary antibody. An Alexa 647-conjugated donkey anti-sheep IgG (1:250x) or goat anti-mouse IgG (ThermoFisher) (1:250x) was used as the secondary antibody. To measure MAC deposition, spirochetes (1 x 10^8 cells) were washed by PBS, resuspended in the same buffer, and then incubated with human or mouse sera in a final concentration as 20% at 25ºC for one hour. Note that more than 80% of *B. burgdorferi* strains are capable of surviving in this concentration of serum (Breitner-Ruddock et al., 1997; Kraiczy, Hunfeld, Breitner-Ruddock, et al., 2000). The spirochetes were then washed with PBS and resuspended in HBSC-DB. A mouse anti-MAC monoclonal antibody aE11 (1:250x) (ThermoFisher), or a rabbit anti-MAC polyclonal IgG (1:250x) (ThermoFisher) was used as the primary antibody. An Alexa 647-conjugated goat anti-rabbit (ThermoFisher) or a goat anti-mouse IgG (ThermoFisher) (1:250x) was used as the secondary antibody.

After staining, formalin (0.1%) was then added for fixing. The resulting fluorescence intensity of spirochetes was measured by flow cytometry using a FACSCalibur (BD Bioscience). All flow cytometry experiments were performed within two days of preparing *B. burgdorferi* samples. Spirochetes in the suspension were distinguished by their distinct light scattering properties in the flow cytometer equipped with a 15mW, 488nm air-cooled argon laser, a standard three-color filter arrangement, and CELLQuest™ Software (BD Bioscience). Unstained

572 *B. burgdorferi* strain B31-A3 was applied to ensure accurate gating, in which the aggregated
573 spirochetes were eliminated as described (Hart, Nguyen, et al., 2018). Additionally, the
574 spirochetes incubated with only the secondary antibody as control experiment to ascertain the
575 specificity of primary antibody to bind to the cognate antigen. The mean fluorescence index
576 (MFI) of each sample was obtained from FlowJo software (Thee-Star Inc., Ashland, OR)
577 representing the surface production of the indicated proteins. Each standard deviation of mean
578 value was no more than 7% of its mean value.
579
580 **Serum susceptibility assay.** The serum susceptibility of *B. burgdorferi* was measured as
581 described (Alitalo et al., 2001). Briefly, triplicate samples of each strain were grown to mid-log
582 phase and diluted to a final concentration of 5×10^6 bacteria per milliliter into BSK-II medium
583 without rabbit serum, plus a final concentration of 40% human or quail serum or C3-depleted
584 human serum (ComTech). We also included heat-inactivated serum from these hosts, which was
585 incubated at 55ºC for two hours prior to incubation with spirochetes. Immediately after and four
586 hours after incubation, an aliquot was taken from each replicate and counted by a Petroff-
587 Hausser counting chamber (Hausser Scientific, Horsham, PA) using a Nikon Eclipse E600
588 darkfield microscope (Nikon, Melville, NY). The percentage of survival for *B. burgdorferi* was
589 calculated using the number of mobile spirochetes at four hours post incubation normalized to
590 that immediately after adding the serum.
591
592 **Mouse and quail infection experiments.** Four-week-old female BALB/c mice or $C3^{-/-}$ mice in a
593 BALB/c background or *Coturnix coturnix* quail were subcutaneously infected with 10^3 (for
594 mouse infection) or 10^6 (for quail infection) of *B. burgdorferi* strains as described (Y. P. Lin et

595 al., 2014). The number of quail and mouse used in each experiment is described in respective
596 figure legends. The plasmid profiles and the presence of the shuttle vector of each of these *B.*
597 *burgdorferi* strains were verified prior to infection as described (Purser & Norris, 2000). Mice
598 were sacrificed at 7 dpi to collect the blood, and 7, or 14 dpi to collect the inoculation site of
599 skin, tibiotarsal joints, bladder, and heart. Quail were sacrificed at 3 and 7 dpi to collect the
600 blood, inoculation site of skin, liver, heart, and brain. Animal tissues were used to quantitatively
601 evaluate the levels of colonization during infection (see section "Quantitative RT-PCR and
602 PCR"). Note that quail blood and tissues were also incubated in BSK-II complete medium at
603 33°C for four weeks to cultivate spirochetes microscopically to verify the viability of spirochetes
604 (Liveris et al., 2002).
605
606 **Statistical analysis.** Significant differences between samples were determined using the
607 Kruskal-Wallis test with Dunn's multiple comparison, or the Mann-Whitney test. A p-value <
608 0.05 was considered to be significant.
609
610 **ACKNOWLEDGEMENTS**
611 We thank Roxie Girardin, John Leong, and Xiuli Yang for valuable technical advice, and
612 Thomas Hart for critical reading of the manuscript. We also thank Utpal Pal for providing *B.*
613 *burgdorferi* strain B31-A3Δ*cspZ*, Jorge Benach for providing the α-FlaB CB1 monoclonal
614 antibody, Susan Madison-Antenucci allowing us to use her fluorescence microscope, and Noel
615 Espina for the assistance with that microscope. Additionally, we thank Leslie Eisele and Renjie
616 Song of Wadsworth Biochemistry and Immunology Core for assistance with circular dichroism
617 and flow cytometry, Karen Chave of the Wadsworth Protein Expression Core for purifying FH

proteins, and Media & Tissue Culture Core for preparation of *Borrelia* and *E. coli* culture medium. This work was supported by NIH R01AI121401 (to P.K. and Y.L.), NSF IOS1755286 (to Y.L., A.L.M., M.Z.C., L.D.K., A.P.D.), DoD TB170111 (to Y.L., M.Z.C., and A.L.M.), NSF DBI1757170 (to M.Z.C.), and New York State Department of Health Wadsworth Center Start-Up Grant (to Y.L., M.Z.C., and A.L.M.). The authors have no conflict of interest to declare.

REFERENCES

Alitalo, A., Meri, T., Comstedt, P., Jeffery, L., Tornberg, J., Strandin, T., . . . Meri, S. (2005). Expression of complement factor H binding immunoevasion proteins in *Borrelia garinii* isolated from patients with neuroborreliosis. *European journal of immunology, 35*(10), 3043-3053. doi:10.1002/eji.200526354

Alitalo, A., Meri, T., Ramo, L., Jokiranta, T. S., Heikkila, T., Seppala, I. J., . . . Meri, S. (2001). Complement evasion by *Borrelia burgdorferi*: serum-resistant strains promote C3b inactivation. *Infection and immunity, 69*(6), 3685-3691. doi:10.1128/IAI.69.6.3685-3691.2001

Antonara, S., Ristow, L., McCarthy, J., & Coburn, J. (2010). Effect of *Borrelia burgdorferi* OspC at the site of inoculation in mouse skin. *Infection and immunity, 78*(11), 4723-4733. doi:10.1128/IAI.00464-10

Benoit, V. M., Fischer, J. R., Lin, Y. P., Parveen, N., & Leong, J. M. (2011). Allelic variation of the Lyme disease spirochete adhesin DbpA influences spirochetal binding to decorin, dermatan sulfate, and mammalian cells. *Infection and immunity, 79*(9), 3501-3509. doi:10.1128/IAI.00163-11

Bhide, M. R., Travnicek, M., Levkutova, M., Curlik, J., Revajova, V., & Levkut, M. (2005). Sensitivity of *Borrelia* genospecies to serum complement from different animals and human: a

641 host-pathogen relationship. *FEMS immunology and medical microbiology, 43*(2), 165-172.
642 doi:10.1016/j.femsim.2004.07.012
643 Bishop, K. L., Khan, M. I., & Nielsen, S. W. (1994). Experimental infection of northern
644 bobwhite quail with *Borrelia burgdorferi*. *Journal of wildlife diseases, 30*(4), 506-513.
645 doi:10.7589/0090-3558-30.4.506
646 Blevins, J. S., Hagman, K. E., & Norgard, M. V. (2008). Assessment of decorin-binding protein
647 A to the infectivity of *Borrelia burgdorferi* in the murine models of needle and tick infection.
648 *BMC microbiology, 8*, 82. doi:10.1186/1471-2180-8-82
649 Blom, A. M., Hallstrom, T., & Riesbeck, K. (2009). Complement evasion strategies of
650 pathogens-acquisition of inhibitors and beyond. *Molecular immunology, 46*(14), 2808-2817.
651 doi:10.1016/j.molimm.2009.04.025
652 Breitner-Ruddock, S., Wurzner, R., Schulze, J., & Brade, V. (1997). Heterogeneity in the
653 complement-dependent bacteriolysis within the species of *Borrelia burgdorferi*. *Medical*
654 *microbiology and immunology, 185*(4), 253-260.
655 Brisson, D., Drecktrah, D., Eggers, C. H., & Samuels, D. S. (2012). Genetics of *Borrelia*
656 *burgdorferi*. *Annual review of genetics, 46*, 515-536. doi:10.1146/annurev-genet-011112-112140
657 Brooks, C. S., Hefty, P. S., Jolliff, S. E., & Akins, D. R. (2003). Global analysis of *Borrelia*
658 *burgdorferi* genes regulated by mammalian host-specific signals. *Infection and immunity, 71*(6),
659 3371-3383.
660 Brooks, C. S., Vuppala, S. R., Jett, A. M., Alitalo, A., Meri, S., & Akins, D. R. (2005).
661 Complement regulator-acquiring surface protein 1 imparts resistance to human serum in *Borrelia*
662 *burgdorferi*. *Journal of immunology, 175*(5), 3299-3308.

663 Burgess, E. C. (1989). Experimental inoculation of mallard ducks (Anas platyrhynchos
664 platyrhynchos) with *Borrelia burgdorferi*. *Journal of wildlife diseases, 25*(1), 99-102.
665 doi:10.7589/0090-3558-25.1.99
666 Bykowski, T., Woodman, M. E., Cooley, A. E., Brissette, C. A., Brade, V., Wallich, R., . . .
667 Stevenson, B. (2007). Coordinated expression of *Borrelia burgdorferi* complement regulator-
668 acquiring surface proteins during the Lyme disease spirochete's mammal-tick infection cycle.
669 *Infection and immunity, 75*(9), 4227-4236. doi:10.1128/IAI.00604-07
670 Caine, J. A., & Coburn, J. (2015). A short-term *Borrelia burgdorferi* infection model identifies
671 tissue tropisms and bloodstream survival conferred by adhesion proteins. *Infection and immunity,*
672 *83*(8), 3184-3194. doi:10.1128/IAI.00349-15
673 Caine, J. A., Lin, Y. P., Kessler, J. R., Sato, H., Leong, J. M., & Coburn, J. (2017). *Borrelia*
674 *burgdorferi* outer surface protein C (OspC) binds complement component C4b and confers
675 bloodstream survival. *Cellular microbiology*. doi:10.1111/cmi.12786
676 Coleman, A. S., Yang, X., Kumar, M., Zhang, X., Promnares, K., Shroder, D., . . . Pal, U.
677 (2008). *Borrelia burgdorferi* complement regulator-acquiring surface protein 2 does not
678 contribute to complement resistance or host infectivity. *PloS one, 3*(8), 3010e.
679 doi:10.1371/journal.pone.0003010
680 Craig-Mylius, K. A., Lee, M., Jones, K. L., & Glickstein, L. J. (2009). Arthritogenicity of
681 *Borrelia burgdorferi* and *Borrelia garinii*: comparison of infection in mice. *The American*
682 *journal of tropical medicine and hygiene, 80*(2), 252-258.
683 Dowdell, A. S., Murphy, M. D., Azodi, C., Swanson, S. K., Florens, L., Chen, S., & Zuckert, W.
684 R. (2017). Comprehensive Spatial Analysis of the *Borrelia burgdorferi* Lipoproteome Reveals a

685 Compartmentalization Bias toward the Bacterial Surface. *Journal of bacteriology, 199*(6).
686 doi:10.1128/JB.00658-16
687 Eisen, R. J., & Eisen, L. (2018). The Blacklegged Tick, *Ixodes scapularis*: An Increasing Public
688 Health Concern. *Trends in parasitology, 34*(4), 295-309. doi:10.1016/j.pt.2017.12.006
689 El-Hage, N., Babb, K., Carroll, J. A., Lindstrom, N., Fischer, E. R., Miller, J. C., . . . Stevenson,
690 B. (2001). Surface exposure and protease insensitivity of *Borrelia burgdorferi* Erp (OspEF-
691 related) lipoproteins. *Microbiology, 147*(Pt 4), 821-830. doi:10.1099/00221287-147-4-821
692 Elias, A. F., Stewart, P. E., Grimm, D., Caimano, M. J., Eggers, C. H., Tilly, K., . . . Rosa, P.
693 (2002). Clonal polymorphism of *Borrelia burgdorferi* strain B31 MI: implications for
694 mutagenesis in an infectious strain background. *Infection and immunity, 70*(4), 2139-2150.
695 Exner, M. M., Wu, X., Blanco, D. R., Miller, J. N., & Lovett, M. A. (2000). Protection elicited
696 by native outer membrane protein Oms66 (p66) against host-adapted *Borrelia burgdorferi*:
697 conformational nature of bactericidal epitopes. *Infection and immunity, 68*(5), 2647-2654.
698 Feng, J., Wang, T., Zhang, S., Shi, W., & Zhang, Y. (2014). An optimized SYBR Green I/PI
699 assay for rapid viability assessment and antibiotic susceptibility testing for *Borrelia burgdorferi*.
700 *PloS one, 9*(11), e111809. doi:10.1371/journal.pone.0111809
701 Frank, K. L., Bundle, S. F., Kresge, M. E., Eggers, C. H., & Samuels, D. S. (2003). aadA confers
702 streptomycin resistance in *Borrelia burgdorferi*. *Journal of bacteriology, 185*(22), 6723-6727.
703 Garcia, B. L., Zhi, H., Wager, B., Hook, M., & Skare, J. T. (2016). *Borrelia burgdorferi* BBK32
704 Inhibits the Classical Pathway by Blocking Activation of the C1 Complement Complex. *PLoS*
705 *pathogens, 12*(1), e1005404. doi:10.1371/journal.ppat.1005404
706 Ginsberg, H. S., Buckley, P. A., Balmforth, M. G., Zhioua, E., Mitra, S., & Buckley, F. G.
707 (2005). Reservoir competence of native North American birds for the lyme disease spirochete,

Borrelia burgdorfieri. *Journal of medical entomology, 42*(3), 445-449. doi:10.1603/0022-2585(2005)042[0445:RCONNA]2.0.CO;2

Hallstrom, T., Haupt, K., Kraiczy, P., Hortschansky, P., Wallich, R., Skerka, C., & Zipfel, P. F. (2010). Complement regulator-acquiring surface protein 1 of *Borrelia burgdorferi* binds to human bone morphogenic protein 2, several extracellular matrix proteins, and plasminogen. *The Journal of infectious diseases, 202*(3), 490-498. doi:10.1086/653825

Hallstrom, T., Siegel, C., Morgelin, M., Kraiczy, P., Skerka, C., & Zipfel, P. F. (2013). CspA from *Borrelia burgdorferi* inhibits the terminal complement pathway. *mBio, 4*(4). doi:10.1128/mBio.00481-13

Hamdy, B. H. (1977). Biochemical and physiological studies of certain ticks (*Ixodoidea*). Excretion during ixodid feeding. *Journal of medical entomology, 14*(1), 15-18.

Hart, T., Nguyen, N. T. T., Nowak, N. A., Zhang, F., Linhardt, R. J., Diuk-Wasser, M., . . . Lin, Y. P. (2018). Polymorphic factor H-binding activity of CspA protects Lyme borreliae from the host complement in feeding ticks to facilitate tick-to-host transmission. *PLoS pathogens, 14*(5), e1007106. doi:10.1371/journal.ppat.1007106

Hart, T., Yang, X., Pal, U., & Lin, Y. P. (2018). Identification of Lyme borreliae proteins promoting vertebrate host blood-specific spirochete survival in Ixodes scapularis nymphs using artificial feeding chambers. *Ticks and tick-borne diseases*. doi:10.1016/j.ttbdis.2018.03.033

Hartmann, K., Corvey, C., Skerka, C., Kirschfink, M., Karas, M., Brade, V., . . . Kraiczy, P. (2006). Functional characterization of BbCRASP-2, a distinct outer membrane protein of *Borrelia burgdorferi* that binds host complement regulators factor H and FHL-1. *Molecular microbiology, 61*(5), 1220-1236. doi:10.1111/j.1365-2958.2006.05318.x

730 Heroldova, M., Nemec, M., & Hubalek, Z. (1998). Growth parameters of *Borrelia burgdorferi*
731 sensu stricto at various temperatures. *Zentralblatt fur Bakteriologie : international journal of*
732 *medical microbiology, 288*(4), 451-455.
733 Hinckley, A. F., Connally, N. P., Meek, J. I., Johnson, B. J., Kemperman, M. M., Feldman, K.
734 A., . . . Mead, P. S. (2014). Lyme disease testing by large commercial laboratories in the United
735 States. *Clinical infectious diseases : an official publication of the Infectious Diseases Society of*
736 *America, 59*(5), 676-681. doi:10.1093/cid/ciu397
737 Hiramatsu, A., & Ouchi, T. (1963). On the Proteolytic Enzymes from the Commercial Protease
738 Preparation of *Streptomyces Griseus* (Pronase P). *Journal of biochemistry, 54*, 462-464.
739 Hodzic, E., Feng, S., & Barthold, S. W. (2013). Assessment of transcriptional activity of
740 *Borrelia burgdorferi* and host cytokine genes during early and late infection in a mouse model.
741 *Vector borne and zoonotic diseases, 13*(10), 694-711. doi:10.1089/vbz.2012.1189
742 Hovius, J. W., Bijlsma, M. F., van der Windt, G. J., Wiersinga, W. J., Boukens, B. J., Coumou,
743 J., . . . van der Poll, T. (2009). The urokinase receptor (uPAR) facilitates clearance of *Borrelia*
744 *burgdorferi*. *PLoS pathogens, 5*(5), e1000447. doi:10.1371/journal.ppat.1000447
745 Hyde, J. A., Trzeciakowski, J. P., & Skare, J. T. (2007). *Borrelia burgdorferi* alters its gene
746 expression and antigenic profile in response to CO_2 levels. *Journal of bacteriology, 189*(2), 437-
747 445. doi:10.1128/JB.01109-06
748 Hyde, J. A., Weening, E. H., Chang, M., Trzeciakowski, J. P., Hook, M., Cirillo, J. D., & Skare,
749 J. T. (2011). Bioluminescent imaging of *Borrelia burgdorferi in vivo* demonstrates that the
750 fibronectin-binding protein BBK32 is required for optimal infectivity. *Molecular microbiology,*
751 *82*(1), 99-113. doi:10.1111/j.1365-2958.2011.07801.x

Isogai, E., Tanaka, S., Braga, I. S., 3rd, Itakura, C., Isogai, H., Kimura, K., & Fujii, N. (1994). Experimental *Borrelia garinii* infection of Japanese quail. *Infection and immunity, 62*(8), 3580-3582.

Jones, K. L., Glickstein, L. J., Damle, N., Sikand, V. K., McHugh, G., & Steere, A. C. (2006). *Borrelia burgdorferi* genetic markers and disseminated disease in patients with early Lyme disease. *Journal of clinical microbiology, 44*(12), 4407-4413. doi:10.1128/JCM.01077-06

Kenedy, M. R., & Akins, D. R. (2011). The OspE-related proteins inhibit complement deposition and enhance serum resistance of *Borrelia burgdorferi*, the lyme disease spirochete. *Infection and immunity, 79*(4), 1451-1457. doi:10.1128/IAI.01274-10

Kenedy, M. R., Lenhart, T. R., & Akins, D. R. (2012). The role of *Borrelia burgdorferi* outer surface proteins. *FEMS immunology and medical microbiology, 66*(1), 1-19. doi:10.1111/j.1574-695X.2012.00980.x

Kenedy, M. R., Vuppala, S. R., Siegel, C., Kraiczy, P., & Akins, D. R. (2009). CspA-mediated binding of human factor H inhibits complement deposition and confers serum resistance in *Borrelia burgdorferi*. *Infection and immunity, 77*(7), 2773-2782. doi:10.1128/IAI.00318-09

Kingry, L. C., Batra, D., Replogle, A., Rowe, L. A., Pritt, B. S., & Petersen, J. M. (2016). Whole Genome Sequence and Comparative Genomics of the Novel Lyme Borreliosis Causing Pathogen, *Borrelia mayonii*. *PloS one, 11*(12), e0168994. doi:10.1371/journal.pone.0168994

Kraiczy, P. (2016a). Hide and Seek: How Lyme Disease Spirochetes Overcome Complement Attack. *Frontiers in immunology, 7*, 385. doi:10.3389/fimmu.2016.00385

Kraiczy, P. (2016b). Travelling between Two Worlds: Complement as a Gatekeeper for an Expanded Host Range of Lyme Disease Spirochetes. *Vet. Sci. , 3*(2), 12-26. doi: doi:10.3390/vetsci3020012

775 Kraiczy, P., Hellwage, J., Skerka, C., Becker, H., Kirschfink, M., Simon, M. M., . . . Wallich, R.
776 (2004). Complement resistance of *Borrelia burgdorferi* correlates with the expression of
777 BbCRASP-1, a novel linear plasmid-encoded surface protein that interacts with human factor H
778 and FHL-1 and is unrelated to Erp proteins. *The Journal of biological chemistry, 279*(4), 2421-
779 2429. doi:10.1074/jbc.M308343200
780 Kraiczy, P., Hunfeld, K. P., Breitner-Ruddock, S., Wurzner, R., Acker, G., & Brade, V. (2000).
781 Comparison of two laboratory methods for the determination of serum resistance in *Borrelia*
782 *burgdorferi* isolates. *Immunobiology, 201*(3-4), 406-419. doi:10.1016/S0171-2985(00)80094-7
783 Kraiczy, P., Hunfeld, K. P., Peters, S., Wurzner, R., Ackert, G., Wilske, B., & Brade, V. (2000).
784 Borreliacidal activity of early Lyme disease sera against complement-resistant *Borrelia afzelii*
785 FEM1 wild-type and an OspC-lacking FEM1 variant. *Journal of medical microbiology, 49*(10),
786 917-928. doi:10.1099/0022-1317-49-10-917
787 Kraiczy, P., Seling, A., Brissette, C. A., Rossmann, E., Hunfeld, K. P., Bykowski, T., . . .
788 Stevenson, B. (2008). *Borrelia burgdorferi* complement regulator-acquiring surface protein 2
789 (CspZ) as a serological marker of human Lyme disease. *Clinical and vaccine immunology : CVI,*
790 *15*(3), 484-491. doi:10.1128/CVI.00415-07
791 Kraiczy, P., Skerka, C., Brade, V., & Zipfel, P. F. (2001). Further characterization of
792 complement regulator-acquiring surface proteins of *Borrelia burgdorferi*. *Infection and*
793 *immunity, 69*(12), 7800-7809. doi:10.1128/IAI.69.12.7800-7809.2001
794 Kraiczy, P., & Stevenson, B. (2013). Complement regulator-acquiring surface proteins of
795 *Borrelia burgdorferi*: Structure, function and regulation of gene expression. *Ticks and tick-borne*
796 *diseases, 4*(1-2), 26-34. doi:10.1016/j.ttbdis.2012.10.039

797 Kumar, D., Ristow, L. C., Shi, M., Mukherjee, P., Caine, J. A., Lee, W. Y., . . . Chaconas, G.
798 (2015). Intravital Imaging of Vascular Transmigration by the Lyme Spirochete: Requirement for
799 the Integrin Binding Residues of the *B. burgdorferi* P66 Protein. *PLoS pathogens, 11*(12),
800 e1005333. doi:10.1371/journal.ppat.1005333
801 Kumru, O. S., Schulze, R. J., Slusser, J. G., & Zuckert, W. R. (2010). Development and
802 validation of a FACS-based lipoprotein localization screen in the Lyme disease spirochete
803 *Borrelia burgdorferi*. *BMC microbiology, 10*, 277. doi:10.1186/1471-2180-10-277
804 Kurtenbach, K., De Michelis, S., Etti, S., Schafer, S. M., Sewell, H. S., Brade, V., & Kraiczy, P.
805 (2002). Host association of *Borrelia burgdorferi* sensu lato--the key role of host complement.
806 *Trends in microbiology, 10*(2), 74-79.
807 Kurtenbach, K., Peacey, M., Rijpkema, S. G., Hoodless, A. N., Nuttall, P. A., & Randolph, S. E.
808 (1998). Differential transmission of the genospecies of *Borrelia burgdorferi* sensu lato by game
809 birds and small rodents in England. *Applied and environmental microbiology, 64*(4), 1169-1174.
810 Kurtenbach, K., Schafer, S. M., Sewell, H. S., Peacey, M., Hoodless, A., Nuttall, P. A., &
811 Randolph, S. E. (2002). Differential survival of Lyme borreliosis spirochetes in ticks that feed on
812 birds. *Infection and immunity, 70*(10), 5893-5895.
813 Lachmann, P. J. (2010). Preparing serum for functional complement assays. *Journal of*
814 *immunological methods, 352*(1-2), 195-197. doi:10.1016/j.jim.2009.11.003
815 Lambris, J. D., Ricklin, D., & Geisbrecht, B. V. (2008). Complement evasion by human
816 pathogens. *Nature reviews. Microbiology, 6*(2), 132-142. doi:10.1038/nrmicro1824
817 Lawrenz, M. B., Hardham, J. M., Owens, R. T., Nowakowski, J., Steere, A. C., Wormser, G. P.,
818 & Norris, S. J. (1999). Human antibody responses to VlsE antigenic variation protein of *Borrelia*
819 *burgdorferi*. *Journal of clinical microbiology, 37*(12), 3997-4004.

Lawrenz, M. B., Wooten, R. M., Zachary, J. F., Drouin, S. M., Weis, J. J., Wetsel, R. A., & Norris, S. J. (2003). Effect of complement component C3 deficiency on experimental Lyme borreliosis in mice. *Infection and immunity, 71*(8), 4432-4440.

Limberger, R. J. (2004). The periplasmic flagellum of spirochetes. *Journal of molecular microbiology and biotechnology, 7*(1-2), 30-40. doi:10.1159/000077867

Lin, T., Gao, L., Zhang, C., Odeh, E., Jacobs, M. B., Coutte, L., . . . Norris, S. J. (2012). Analysis of an ordered, comprehensive STM mutant library in infectious *Borrelia burgdorferi*: insights into the genes required for mouse infectivity. *PloS one, 7*(10), e47532. doi:10.1371/journal.pone.0047532

Lin, Y. P., Benoit, V., Yang, X., Martinez-Herranz, R., Pal, U., & Leong, J. M. (2014). Strain-specific variation of the decorin-binding adhesin DbpA influences the tissue tropism of the lyme disease spirochete. *PLoS pathogens, 10*(7), e1004238. doi:10.1371/journal.ppat.1004238

Lin, Y. P., Chen, Q., Ritchie, J. A., Dufour, N. P., Fischer, J. R., Coburn, J., & Leong, J. M. (2015). Glycosaminoglycan binding by *Borrelia burgdorferi* adhesin BBK32 specifically and uniquely promotes joint colonization. *Cellular microbiology, 17*(6), 860-875. doi:10.1111/cmi.12407

Lin, Y. P., Greenwood, A., Nicholson, L. K., Sharma, Y., McDonough, S. P., & Chang, Y. F. (2009). Fibronectin binds to and induces conformational change in a disordered region of leptospiral immunoglobulin-like protein B. *The Journal of biological chemistry, 284*(35), 23547-23557. doi:10.1074/jbc.M109.031369

Liveris, D., Wang, G., Girao, G., Byrne, D. W., Nowakowski, J., McKenna, D., . . . Schwartz, I. (2002). Quantitative detection of *Borrelia burgdorferi* in 2-millimeter skin samples of erythema

migrans lesions: correlation of results with clinical and laboratory findings. *Journal of clinical microbiology, 40*(4), 1249-1253.

Marcinkiewicz, A., Kraiczy, P., & Lin, Y.-P. (2017). There is a method to the madness: Strategies to study host complement evasion by Lyme disease and relapsing fever spirochetes. *Frontiers in microbiology, 8*(328). doi:10.3389/fmicb.2017.00328

Marcinkiewicz, A. L., Lieknina, I., Kotelovica, S., Yang, X., Kraiczy, P., Pal, U., . . . Tars, K. (2018). Eliminating Factor H-Binding Activity of *Borrelia burgdorferi* CspZ Combined with Virus-Like Particle Conjugation Enhances Its Efficacy as a Lyme Disease Vaccine. *Frontiers in immunology, 9*, 181. doi:10.3389/fimmu.2018.00181

McDowell, J. V., Frederick, J., Miller, D. P., Goetting-Minesky, M. P., Goodman, H., Fenno, J. C., & Marconi, R. T. (2011). Identification of the primary mechanism of complement evasion by the periodontal pathogen, *Treponema denticola*. *Molecular oral microbiology, 26*(2), 140-149. doi:10.1111/j.2041-1014.2010.00598.x

McDowell, J. V., Wolfgang, J., Tran, E., Metts, M. S., Hamilton, D., & Marconi, R. T. (2003). Comprehensive analysis of the factor h binding capabilities of borrelia species associated with lyme disease: delineation of two distinct classes of factor h binding proteins. *Infection and immunity, 71*(6), 3597-3602.

Meri, S. (2016). Self-nonself discrimination by the complement system. *FEBS letters, 590*(15), 2418-2434. doi:10.1002/1873-3468.12284

Merle, N. S., Church, S. E., Fremeaux-Bacchi, V., & Roumenina, L. T. (2015). Complement System Part I - Molecular Mechanisms of Activation and Regulation. *Frontiers in immunology, 6*, 262. doi:10.3389/fimmu.2015.00262

Merle, N. S., Noe, R., Halbwachs-Mecarelli, L., Fremeaux-Bacchi, V., & Roumenina, L. T. (2015). Complement System Part II: Role in Immunity. *Frontiers in immunology, 6*, 257. doi:10.3389/fimmu.2015.00257

Moriarty, T. J., Shi, M., Lin, Y. P., Ebady, R., Zhou, H., Odisho, T., . . . Chaconas, G. (2012). Vascular binding of a pathogen under shear force through mechanistically distinct sequential interactions with host macromolecules. *Molecular microbiology, 86*(5), 1116-1131. doi:10.1111/mmi.12045

Morrison, T. B., Ma, Y., Weis, J. H., & Weis, J. J. (1999). Rapid and sensitive quantification of *Borrelia burgdorferi*-infected mouse tissues by continuous fluorescent monitoring of PCR. *Journal of clinical microbiology, 37*(4), 987-992.

Norman, M. U., Moriarty, T. J., Dresser, A. R., Millen, B., Kubes, P., & Chaconas, G. (2008). Molecular mechanisms involved in vascular interactions of the Lyme disease pathogen in a living host. *PLoS pathogens, 4*(10), e1000169. doi:10.1371/journal.ppat.1000169

Ojaimi, C., Brooks, C., Casjens, S., Rosa, P., Elias, A., Barbour, A., . . . Schwartz, I. (2003). Profiling of temperature-induced changes in *Borrelia burgdorferi* gene expression by using whole genome arrays. *Infection and immunity, 71*(4), 1689-1705.

Olsen, B., Gylfe, A., & Bergstrom, S. (1996). Canary finches (*Serinus canaria*) as an avian infection model for Lyme borreliosis. *Microbial pathogenesis, 20*(6), 319-324. doi:10.1006/mpat.1996.0030

Parveen, N., & Leong, J. M. (2000). Identification of a candidate glycosaminoglycan-binding adhesin of the Lyme disease spirochete *Borrelia burgdorferi*. *Molecular microbiology, 35*(5), 1220-1234.

886 Piesman, J., Dolan, M. C., Schriefer, M. E., & Burkot, T. R. (1996). Ability of experimentally
887 infected chickens to infect ticks with the Lyme disease spirochete, *Borrelia burgdorferi*. *The*
888 *American journal of tropical medicine and hygiene, 54*(3), 294-298.
889 Purser, J. E., & Norris, S. J. (2000). Correlation between plasmid content and infectivity in
890 *Borrelia burgdorferi*. *Proceedings of the National Academy of Sciences of the United States of*
891 *America, 97*(25), 13865-13870. doi:10.1073/pnas.97.25.13865
892 Radolf, J. D., Caimano, M. J., Stevenson, B., & Hu, L. T. (2012). Of ticks, mice and men:
893 understanding the dual-host lifestyle of Lyme disease spirochaetes. *Nature reviews.*
894 *Microbiology, 10*(2), 87-99. doi:10.1038/nrmicro2714
895 Revel, A. T., Talaat, A. M., & Norgard, M. V. (2002). DNA microarray analysis of differential
896 gene expression in *Borrelia burgdorferi*, the Lyme disease spirochete. *Proceedings of the*
897 *National Academy of Sciences of the United States of America, 99*(3), 1562-1567.
898 doi:10.1073/pnas.032667699
899 Richter, D., Spielman, A., Komar, N., & Matuschka, F. R. (2000). Competence of American
900 robins as reservoir hosts for Lyme disease spirochetes. *Emerging infectious diseases, 6*(2), 133-
901 138. doi:10.3201/eid0602.000205
902 Ristow, L. C., Miller, H. E., Padmore, L. J., Chettri, R., Salzman, N., Caimano, M. J., . . .
903 Coburn, J. (2012). The beta(3)-integrin ligand of *Borrelia burgdorferi* is critical for infection of
904 mice but not ticks. *Molecular microbiology, 85*(6), 1105-1118. doi:10.1111/j.1365-
905 2958.2012.08160.x
906 Roantree, R. J., & Rantz, L. A. (1960). A Study of the Relationship of the Normal Bactericidal
907 Activity of Human Serum to Bacterial Infection. *The Journal of clinical investigation, 39*(1), 72-
908 81. doi:10.1172/JCI104029

Rogers, E. A., Abdunnur, S. V., McDowell, J. V., & Marconi, R. T. (2009). Comparative analysis of the properties and ligand binding characteristics of CspZ, a factor H binding protein, derived from *Borrelia burgdorferi* isolates of human origin. *Infection and immunity, 77*(10), 4396-4405. doi:10.1128/IAI.00393-09

Rogers, E. A., & Marconi, R. T. (2007). Delineation of species-specific binding properties of the CspZ protein (BBH06) of Lyme disease spirochetes: evidence for new contributions to the pathogenesis of *Borrelia* spp. *Infection and immunity, 75*(11), 5272-5281. doi:10.1128/IAI.00850-07

Samuels, D. S. (1995). Electrotransformation of the spirochete *Borrelia burgdorferi*. *Methods in molecular biology, 47*, 253-259. doi:10.1385/0-89603-310-4:253

Seshu, J., Boylan, J. A., Gherardini, F. C., & Skare, J. T. (2004). Dissolved oxygen levels alter gene expression and antigen profiles in *Borrelia burgdorferi*. *Infection and immunity, 72*(3), 1580-1586.

Seshu, J., Esteve-Gassent, M. D., Labandeira-Rey, M., Kim, J. H., Trzeciakowski, J. P., Hook, M., & Skare, J. T. (2006). Inactivation of the fibronectin-binding adhesin gene *bbk32* significantly attenuates the infectivity potential of *Borrelia burgdorferi*. *Molecular microbiology, 59*(5), 1591-1601. doi:10.1111/j.1365-2958.2005.05042.x

Shi, Y., Xu, Q., Seemanaplli, S. V., McShan, K., & Liang, F. T. (2008). Common and unique contributions of decorin-binding proteins A and B to the overall virulence of *Borrelia burgdorferi*. *PloS one, 3*(10), e3340. doi:10.1371/journal.pone.0003340

Showman, A. C., Aranjuez, G., Adams, P. P., & Jewett, M. W. (2016). Gene *bb0318* Is Critical for the Oxidative Stress Response and Infectivity of *Borrelia burgdorferi*. *Infection and immunity, 84*(11), 3141-3151. doi:10.1128/IAI.00430-16

Siegel, C., Schreiber, J., Haupt, K., Skerka, C., Brade, V., Simon, M. M., . . . Kraiczy, P. (2008). Deciphering the ligand-binding sites in the *Borrelia burgdorferi* complement regulator-acquiring surface protein 2 required for interactions with the human immune regulators factor H and factor H-like protein 1. *The Journal of biological chemistry, 283*(50), 34855-34863. doi:10.1074/jbc.M805844200

Sjoberg, A. P., Trouw, L. A., & Blom, A. M. (2009). Complement activation and inhibition: a delicate balance. *Trends in immunology, 30*(2), 83-90. doi:10.1016/j.it.2008.11.003

Sojka, D., Franta, Z., Horn, M., Caffrey, C. R., Mares, M., & Kopacek, P. (2013). New insights into the machinery of blood digestion by ticks. *Trends in parasitology, 29*(6), 276-285. doi:10.1016/j.pt.2013.04.002

Steere, A. C., Strle, F., Wormser, G. P., Hu, L. T., Branda, J. A., Hovius, J. W., . . . Mead, P. S. (2016). Lyme borreliosis. *Nature reviews. Disease primers, 2*, 16090. doi:10.1038/nrdp.2016.90

Tilly, K., Krum, J. G., Bestor, A., Jewett, M. W., Grimm, D., Bueschel, D., . . . Rosa, P. (2006). *Borrelia burgdorferi* OspC protein required exclusively in a crucial early stage of mammalian infection. *Infection and immunity, 74*(6), 3554-3564. doi:10.1128/IAI.01950-05

Tokarz, R., Anderton, J. M., Katona, L. I., & Benach, J. L. (2004). Combined effects of blood and temperature shift on *Borrelia burgdorferi* gene expression as determined by whole genome DNA array. *Infection and immunity, 72*(9), 5419-5432. doi:10.1128/IAI.72.9.5419-5432.2004

van Dam, A. P., Oei, A., Jaspars, R., Fijen, C., Wilske, B., Spanjaard, L., & Dankert, J. (1997). Complement-mediated serum sensitivity among spirochetes that cause Lyme disease. *Infection and immunity, 65*(4), 1228-1236.

Wang, G., van Dam, A. P., Schwartz, I., & Dankert, J. (1999). Molecular typing of *Borrelia burgdorferi* sensu lato: taxonomic, epidemiological, and clinical implications. *Clinical microbiology reviews, 12*(4), 633-653.

Weening, E. H., Parveen, N., Trzeciakowski, J. P., Leong, J. M., Hook, M., & Skare, J. T. (2008). *Borrelia burgdorferi* lacking DbpBA exhibits an early survival defect during experimental infection. *Infection and immunity, 76*(12), 5694-5705. doi:10.1128/IAI.00690-08

Wickramasekara, S., Bunikis, J., Wysocki, V., & Barbour, A. G. (2008). Identification of residual blood proteins in ticks by mass spectrometry proteomics. *Emerging infectious diseases, 14*(8), 1273-1275. doi:10.3201/eid1408.080227

Wilhelm, D. L. (1973). Mechanisms responsible for increased vascular permeability in acute inflammation. *Agents and actions, 3*(5), 297-306.

Woodman, M. E., Cooley, A. E., Miller, J. C., Lazarus, J. J., Tucker, K., Bykowski, T., . . . Stevenson, B. (2007). *Borrelia burgdorferi* binding of host complement regulator factor H is not required for efficient mammalian infection. *Infection and immunity, 75*(6), 3131-3139. doi:10.1128/IAI.01923-06

Xu, Q., Seemanapalli, S. V., Reif, K. E., Brown, C. R., & Liang, F. T. (2007). Increasing the recruitment of neutrophils to the site of infection dramatically attenuates *Borrelia burgdorferi* infectivity. *Journal of immunology, 178*(8), 5109-5115.

Yang, X. F., Pal, U., Alani, S. M., Fikrig, E., & Norgard, M. V. (2004). Essential role for OspA/B in the life cycle of the Lyme disease spirochete. *The Journal of experimental medicine, 199*(5), 641-648. doi:10.1084/jem.20031960

Zhi, H., Weening, E. H., Barbu, E. M., Hyde, J. A., Hook, M., & Skare, J. T. (2015). The BBA33 lipoprotein binds collagen and impacts *Borrelia burgdorferi* pathogenesis. *Molecular microbiology*. doi:10.1111/mmi.12921

Zhi, H., Xie, J., & Skare, J. T. (2018). The Classical Complement Pathway Is Required to Control *Borrelia burgdorferi* Levels During Experimental Infection. *Frontiers in immunology, 9*, 959. doi:10.3389/fimmu.2018.00959

Zipfel, P. F., & Skerka, C. (2009). Complement regulators and inhibitory proteins. *Nature reviews. Immunology, 9*(10), 729-740. doi:10.1038/nri2620

Zuckert, W. R., Kerentseva, T. A., Lawson, C. L., & Barbour, A. G. (2001). Structural conservation of neurotropism-associated VspA within the variable *Borrelia* Vsp-OspC lipoprotein family. *The Journal of biological chemistry, 276*(1), 457-463. doi:10.1074/jbc.M008449200

997 **Table 1**. **CspZ-Y207A/Y211A does not bind to Factor H from human or quail.**

Recombinant CspZ proteins	Factor H source	K_D (μM)
GST-CspZ	Human	0.29±0.07
	Quail	0.91±0.14
GST-CspZ-Y207A/Y211A	Human	n.b.[a]
	Quail	n.b.
GST[b]	Human	n.b.
	Quail	n.b.

998 All values represent the mean ± SEM of three experiments determined by ELISA.

999 [a] No binding activity was detected.

1000 [b] GST was included as a negative control.

1001

1002

1003

1004

1005

1006

1007

1008

1009

1010

1011

1012

1013

1014

1015

1016 **Table 2. Strains and plasmids used in this study.**

Strain or plasmid	Genotype or characteristic	Source
B. burgdorferi		
B313	High-passage *B. burgdorferi* B31 missing lp5, lp17, lp21, lp25, lp28-1, lp28-2, lp28-3, lp28-4, lp36, lp38, lp54, lp56, cp9, cp32-4, cp32-6, cp32-8, cp32-9	(Hallstrom et al., 2013)
B31-A3	Clone of *B. burgdorferi* B31 missing cp9	(Elias et al., 2002)
B31-A3Δ*cspZ*	B31-A3Δ*cspZ*::KanR[a]	(Coleman et al., 2008)
B31-A3Δ*cspZ*/pKFSS-1	B31-A3Δ*cspZ*::KanR carrying plasmid pKFSS-1	This study
B31-A3Δ*cspZ*/pCspZ-WT	B31-A3Δ*cspZ*::KanR complemented with intact *cspZ*	This study
B31-A3Δ*cspZ*/pCspZ-Y207A/Y211A	B31-A3Δ*cspZ*::KanR complemented with intact *cspZ-Y207A/Y211A*	This study
E. coli		
DH5α	F- Φ80lacZΔM15 Δ(lacZYA-argF) U169 recA1 endA1 hsdR17(rk-, mk+) phoA supE44 thi-1 gyrA96 relA1 λ-	ThermoFisher
BL21(DE3)	F−, ompT hsdSB (rB− mB−) gal dcm (DE3)	Novagen
BL21(DE3)/pGEX4T2-CspZ	BL21(DE3) producing GST-tagged residues 19 to 237 of CspZ	This study
BL21(DE3)/pGEX4T2-CspZ-Y207A/Y211A	BL21(DE3) producing GST-tagged residues 19 to 237 of CspZ-Y207A/Y211A	This study
Plasmids		
pJET1.2/Blunt	AmpR[b]; PCR cloning vector	ThermoFisher
pGEX4T2	AmpR; GST-tagged protein expression vector	Qiagen
pGEX4T2-CspZ	AmpR; pGEX4T2 encoding GST fusion protein residue 19 to 237 of CspZ	This study
pGEX4T2-CspZ-Y207A/Y211A	AmpR; pGEX4T2 encoding GST fusion protein residue 19 to 237 of CspZ-Y207A/Y211A	This study

pKFSS-1	StrR[c]; Borrelia shuttle vector	(Frank et al., 2003)
pKFSS-1/pCspZ-WT	StrR; pKFSS-1 encoding intact *cspZ*	This study
pKFSS-1/pCspZ-Y207A/Y211A	StrR; pKFSS-1 encoding intact *cspZ*-Y207A/Y211A	This study

[a] Kanamycin resistant
[b] Ampicillin resistant
[c] Streptomycin resistant

FIGURE LEGENDS

Figure 1. The surface production of CspZ was enhanced in human blood-treated *B. burgdorferi* compared to untreated spirochetes. Approximately $5x10^6$ cells of the *B. burgdorferi* strain B31-A3 were cultivated in BSK-II medium with or without ("Untreated") 5% blood ("Blood") for 48 hours. **(A)** RNA from blood-treated or untreated spirochetes was extracted. The expression levels of *cspZ*, the constitutively expressed genes *16s rRNA,* and *recA* were determined using qRT-PCR. The expression levels of *recA* (control) and *cspZ* are presented by normalizing to the expression levels of the gene encoding *16s rRNA*. Each bar represents the mean of four independent determinations ± SEM. The asterisk ("*") indicates significant differences ($p < 0.05$; Mann-Whitney test) in the normalized expression levels of *cspZ* in blood-treated spirochetes relative to that of untreated spirochetes. **(B)** Representative histograms of flow cytometry analysis showing the levels of CspZ surface production to blood-treated or untreated spirochetes. The shaded histograms are derived from untreated or blood-treated spirochetes incubated only with Alexa 647-conjugated goat anti-mouse IgG as control. **(C to F)** The production of FlaB (negative control), CspA or CspZ on the surface of blood-treated or untreated spirochetes was detected by flow cytometry. The mean fluorescence index ("MFI") represents the production levels of FlaB, CspA, or CspZ in unpermeablized (filled bars) or methanol-permeabilized (opened bars) **(C)** *B. burgdorferi* strain B31-A3, **(D)** B31-A3Δ*cspZ* harboring the vector pKFSS-1 ("B31-A3Δ*cspZ*/Vector"), or **(E)** this *cspZ* mutant strain producing CspZ ("B31-A3Δ*cspZ*/pCspZ") or **(F)** CspZ-Y207A/Y211A ("B31-A3Δ*cspZ*/pCspZ-Y207A/Y211A"). Each bar represents the mean of four independent determinations ± the standard deviation. The asterisk ("*") indicates significantly different protein production ($p < 0.05$ by Kruskal-Wallis test with Dunn's multiple comparison) between blood-treated and

untreated indicated *B. burgdorferi* strains. Note that the production of FlaB, CspA, or CspZ among different spirochete strains when these strains were in blood-treated or untreated conditions is no different ($p > 0.05$ by Kruskal-Wallis test with Dunn's multiple comparison).

Figure 2. Tyrosine-207 and -211 of CspZ were critical for blood-treated *B. burgdorferi* to bind to human, mouse, and quail FH. Human blood-treated *B. burgdorferi* strain B313, B31-A3, B31-A3Δ*cspZ* harboring the vector pKFSS-1 ("B31-A3Δ*cspZ*/Vector"), or this *cspZ* mutant strain producing CspZ ("B31-A3Δ*cspZ*/pCspZ") or CspZ-Y207A/Y211A ("B31-A3Δ*cspZ*/pCspZ-Y207A/Y211A") was incubated with either PBS (negative control, data not shown) or FH from human, mouse, or quail. The bacteria were stained with a sheep anti-FH polyclonal IgG (for the spirochetes incubated with human or mouse FH) or a mouse anti-FH monoclonal antibody VIG8 (for the spirochetes incubated with quail FH) followed by an Alexa 647-conjugated donkey anti-sheep IgG or goat anti-mouse IgG prior to flow cytometry analysis. **(Left panel)** Representative histograms of flow cytometry analysis showing the levels of FH from **(A)** human, **(B)** mouse, or **(C)** quail binding to the indicated *B. burgdorferi* strains. **(Right panel)** The levels of *B. burgdorferi* binding to FH from **(A)** human, **(B)** mouse, or **(C)** quail were measured by flow cytometry and presented as mean fluorescence index ("MFI"). Each bar represents the mean of three independent determinations ± SEM. Significant differences ($p < 0.05$ by Kruskal-Wallis test with Dunn's multiple comparison) in the levels of FH binding relative to the strain B313 ("Φ"), the strain Δ*cspZ*/Vector ("*"), or between two strains relative to each other ("#") are indicated.

Figure 3. CspZ-mediated FH-binding activity decreased MAC deposition on the surface of blood-treated *B. burgdorferi*. Human blood-treated *B. burgdorferi* strain B313, B31-A3, B31-A3Δ*cspZ* harboring the vector pKFSS-1 ("B31-A3Δ*cspZ*/Vector"), or this *cspZ* mutant strain producing CspZ ("B31-A3Δ*cspZ*/pCspZ") or CspZ-Y207A/Y211A ("B31-A3Δ*cspZ*/pCspZ-Y207A/Y211A") was incubated with either PBS (negative control, data not shown) or serum from human or mouse at a final concentration of 20%. The bacteria were stained with a mouse anti-MAC monoclonal antibody aE11 (for spirochetes incubated with human serum), or a rabbit anti-MAC polyclonal IgG (for spirochetes incubated with mouse serum) followed by a goat anti-mouse IgG, or a goat anti-rabbit IgG, prior to flow cytometry analysis. **(A)** Representative histograms of flow cytometry analysis showing the deposition levels of mouse MAC on the surface of indicated *B. burgdorferi* strains. **(B)** The deposition levels of human or mouse MAC on the surface of *B. burgdorferi* were measured by flow cytometry and presented as mean fluorescence index ("MFI"). Each bar represents the mean of three independent determinations ± SEM. Significant differences ($p < 0.05$ by Kruskal-Wallis test with Dunn's multiple comparison) in the deposition levels of MAC relative to the strain B313 ("Φ"), the strain B31-A3Δ*cspZ*/Vector ("*"), or between two strains relative to each other ("#") are indicated.

Figure 4. CspZ-mediated FH-binding activity contributed to the survival of blood-treated spirochetes in human and quail serum. Human blood-treated *B. burgdorferi* strain B31-A3, B31-A3Δ*cspZ* harboring the vector pKFSS-1 ("B31-A3Δ*cspZ*/Vector"), or this *cspZ* mutant strain producing CspZ ("B31-A3Δ*cspZ*/pCspZ") or CspZ-Y207A/Y211A ("B31-A3Δ*cspZ*/pCspZ-Y207A/Y211A") was incubated for four hours with untreated (filled bars) or heat-inactivated ("Heat-treated", hatched bars) serum at a final concentration of 40%. These sera

include **(A)** normal human serum, **(B)** C3-depleted human serum ("Human $C3^-$ serum"), or **(C)** quail serum. The number of motile spirochetes was assessed microscopically. The percentage of surviving *B. burgdorferi* was calculated using the number of mobile spirochetes at four hours post incubation normalized to that immediately after incubation with serum. Each bar represents the mean of three independent determinations ± SEM. Significant differences ($p < 0.05$ by Kruskal-Wallis test with Dunn's multiple comparison) in the percentage of surviving spirochetes relative to the strain B31-A3Δ*cspZ*/Vector incubated with untreated serum ("*") or between two strains relative to each other ("#") are indicated.

Figure 5. CspZ-mediated FH-binding activity promoted bacteremia and tissue colonization of blood-treated *B. burgdorferi* in mice. BALB/c mice were subcutaneously infected with 10^3 cells of human blood-treated *B. burgdorferi* strain B31-A3, B31-A3Δ*cspZ* harboring the vector pKFSS-1 ("B31-A3Δ*cspZ*/Vector"), or this *cspZ* mutant strain producing CspZ ("B31-A3Δ*cspZ*/pCspZ") or CspZ-Y207A/Y211A ("B31-A3Δ*cspZ*/pCspZ-Y207A/Y211A"). These mice were sacrificed at **(left panel)** 7 or **(right panel)** 14 days post-infection ("dpi"). The spirochete burdens in the **(A)** Blood, **(B)** inoculation site of skin ("Inoc. Site"), **(C)** heart, **(D)** bladder, and **(E)** tibiotarsus joints were determined by qPCR and normalized to 1µg total DNA. Shown are the geometric mean ± geometric standard deviation of 14 (blood from B31-A3-infected mice at 7dpi), 15 (blood from B31-A3Δ*cspZ*/Vector- or B31-A3Δ*cspZ*/pCspZ-Y207A/Y211A-infected mice at 7dpi), 12 (blood from B31-A3Δ*cspZ*/pCspZ-infected mice at 7dpi), 6 (blood from B31-A3-infected mice at 14 dpi), 8 (tibiotarsus joints from B31-A3-infected mice), 16 (Inoc. Site from B31-A3- or B31-A3Δ*cspZ*/pCspZ-infected mice at 14dpi), 9 (bladder or heart from B31-A3-infected mice at 14dpi), 7 (blood from B31-A3Δ*cspZ*/Vector-infected

mice or bladder or heart from B31-A3Δ*cspZ*/pCspZ-infected mice at 14dpi) or 10 (all others) mice per group. Significant differences ($p < 0.05$ by Kruskal-Wallis test with Dunn's multiple comparison) in the spirochete burdens relative to the strain B31-A3Δ*cspZ*/Vector ("*") or between two strains relative to each other ("#") are indicated. ("n.d."): not determined.

Figure 6. CspZ-mediated FH-binding activity facilitated bacteremia and tissue colonization of blood-treated spirochetes by evading the mouse complement. BALB/c $C3^{-/-}$ mice were subcutaneously infected with 10^3 cells of human blood-treated *B. burgdorferi* strain B31-A3, B31-A3Δ*cspZ* harboring the vector pKFSS-1 ("B31-A3Δ*cspZ*/Vector"), or this *cspZ* mutant strain producing CspZ ("B31-A3Δ*cspZ*/pCspZ") or CspZ-Y207A/Y211A ("B31-A3Δ*cspZ*/pCspZ-Y207A/Y211A"). The mice were sacrificed at **(left panel)** 7 or **(right panel)** 14 days post-infection ("dpi"). The spirochete burdens in the **(A)** blood, **(B)** inoculation site of skin ("Inoc Site"), **(C)** heart, **(D)** bladder, and **(E)** tibiotarsus joints were determined by qPCR and normalized to 1μg total DNA. Shown are the geometric mean ± geometric standard deviation of 5 (tibiotarsus joints from B31-A3Δ*cspZ*/pCspZ-Y207A/Y211A-infected mice at 7dpi) or 6 (all others) mice per group. There were no significant differences ($p < 0.05$ by Kruskal-Wallis test with Dunn's multiple comparison) in the spirochete burdens relative to the strain B31-A3Δ*cspZ*/Vector or between two strains relative to each other.

Figure 7. CspZ-mediated FH-binding activity promoted *B. burgdorferi* colonization in quail. *Coturnix coturnix* quail were subcutaneously infected with 10^6 cells of human blood-treated *B. burgdorferi* strain B31-A3, B31-A3Δ*cspZ* harboring the vector pKFSS-1 ("B31-A3Δ*cspZ*/Vector"), or this *cspZ* mutant strain producing CspZ ("B31-A3Δ*cspZ*/pCspZ") or

CspZ-Y207A/Y211A ("B31-A3Δ*cspZ*/pCspZ-Y207A/Y211A"). The quail were sacrificed at seven days post-infection ("dpi"). The spirochete burdens in the **(A)** inoculation site of skin ("Inoc. Site") and **(B)** brain were determined by qPCR and normalized to 1µg total DNA. Shown are the geometric mean ± geometric standard deviation of 8 (B31-A3-infected quail), 14 (Inoc. Site from B31-A3Δ*cspZ*/pCspZ-infected quail), 9 (brain from B31-A3Δ*cspZ*/pCspZ-infected quail), 6 (all others) quail per group. Significant differences ($p < 0.05$ by Kruskal-Wallis test with Dunn's multiple comparison) in the spirochete burdens relative to the strain B31-A3Δ*cspZ*/Vector ("*") or between two strains relative to each other ("#") are indicated.

SUPPLEMENTARY MATERIAL

SUPPLEMENTAL FIGURE LEGENDS

Figure S1. Recombinant CspZ but not CspZ-Y207A/Y211A bound to human and quail FH. The indicated concentrations of GST-tagged CspZ ("CspZ") or CspZ-Y207A/Y211A, or GST were added in triplicate to wells coated with 1µg of BSA (negative control, data not shown), or human or quail FH, and protein binding was quantified by ELISA. The experiments were performed on three independent occasions; in each experiment, samples were run in duplicate. All experiments were performed with a single preparation of recombinant proteins. Shown is a representative experiment from the average of two replicates. The K_D values (Table 1) representing the FH-binding affinity of each protein were determined from the average of three experiments.

Figure S2. Substitution of tyrosine-207 and -211 with alanine in CspZ did not affect its structure. Far-UV CD analysis of CspZ and CspZ-Y207A/Y211A. The molar ellipticity, Φ, was measured from 190-250nm for 10µM of each protein in PBS buffer.

Figure S3. Substitution of tyrosine-207 and -211 with alanine in CspZ did not affect its ability to bind fibronectin, plasminogen, and laminin. The indicated concentrations of various recombinant GST-tagged CspZ ("CspZ") or CspZ-Y207A/Y211A, or GST (negative control) were added in triplicate to wells coated with 1µg of BSA (negative control, data not shown), **(top panel)** fibronectin, **(middle panel)** plasminogen, or **(bottom panel)** laminin. The protein binding was quantified by ELISA. The experiments were performed on three independent occasions; within each occasion, samples were run in triplicate. Shown is one representative experiment

with mean ± SEM of three replicates in that particular experiment. The K_D values of mean ± SEM of three experiments for the fibronectin-, plasminogen-, and laminin-binding activity of CspZ and CspZ-Y207A/Y211A were shown in the tables at the top of each panel. There was no significant difference ($p > 0.05$; Mann-Whitney test) between the affinity of CspZ and CspZ-Y207A/Y211A in binding to fibronectin, plasminogen, or laminin.

Figure S4. Determination of the viability and generation times of blood-treated and untreated *B. burgdorferi* strains. 10^6 cells of *B. burgdorferi* strain B31-A3, B31-A3Δ*cspZ* harboring the vector pKFSS-1 ("B31-A3Δ*cspZ*/Vector"), or this *cspZ* mutant strain producing CspZ ("B31-A3Δ*cspZ*/pCspZ") or CspZ-Y207A/Y211A ("B31-A3Δ*cspZ*/pCspZ-Y207A/Y211A") were treated with human blood ("Blood-treated"). Untreated strains were included as control. **(A)** At 48 hours post treatment, the spirochetes were washed and stained by SYBR Green and propidium iodide to evaluate their viability under fluorescence microscopy. The experiments were performed on three independent occasions; within each occasion, the number of bacteria was counted from four fields of view. Shown are representative micrographs. The percentage of live spirochetes is presented in the Table S2. There were no significant differences ($p > 0.05$ with Kruskal-Wallis test and Dunn's multiple comparison) in the viability between any strains. **(B and C)** At 48 hours post treatment, the spirochetes were washed and cultivated in fresh BSK-II medium at 33°C. The concentration of each of these strains was quantified microscopically at the indicated time points. The experiments were performed on three independent occasions; within each occasion, the number of bacteria was counted from three fields. Shown are the geometric mean number of spirochetes ± geometric standard deviation of three different experiments. The generation time was calculated and shown in the

Table S3. There were no significant differences ($p > 0.05$ with Kruskal-Wallis test and Dunn's multiple comparison) in the generation time between any strains.

Figure S5. CspZ is not essential for untreated *B. burgdorferi* to bound to human, mouse, and quail FH. Untreated *B. burgdorferi* strain B313, B31-A3, or B31-A3Δ*cspZ* harboring the vector pKFSS-1 ("B31-A3Δ*cspZ*/Vector") was incubated with either PBS (negative control, data not shown) or FH from human, mouse, or quail. The bacteria were stained with a sheep anti-FH polyclonal IgG (for the spirochetes incubated with human or mouse FH) or a mouse anti-FH monoclonal antibody VIG8 (for the spirochetes incubated with quail FH) followed by an Alexa 647-conjugated donkey anti-sheep IgG or goat anti-mouse IgG prior to flow cytometry analysis. **(Left panel)** Representative histograms of flow cytometry analysis showing the levels of FH from **(A)** human, **(B)** mouse, or **(C)** quail binding to the indicated *B. burgdorferi* strains. **(Right panel)** The levels of *B. burgdorferi* binding to FH from **(A)** human, **(B)** mouse, or **(C)** quail were measured by flow cytometry and presented as mean fluorescence index ("MFI"). Each bar represents the mean of three independent determinations ± SEM. Significant differences ($p < 0.05$ by Kruskal-Wallis test with Dunn's multiple comparison) in the levels of FH binding relative to the strain B313 ("Φ") are indicated.

Figure S6. CspZ was not required to reduce the levels of MAC deposition on the surface of untreated *B. burgdorferi*. Untreated *B. burgdorferi* strain B313, B31-A3, or B31-A3Δ*cspZ* harboring the vector pKFSS-1 ("B31-A3Δ*cspZ*/Vector") was incubated with either PBS (negative control, data not shown) or serum from human or mouse at a final concentration of 20%. The bacteria were stained with a mouse anti-MAC monoclonal antibody aE11 (for

spirochetes incubated with human serum), or a rabbit anti-MAC polyclonal IgG (for spirochetes incubated with mouse serum) followed by a goat anti-mouse IgG, or a goat anti-rabbit IgG, prior to flow cytometry analysis. **(A)** Representative histograms of flow cytometry analysis showing the deposition levels of mouse MAC on the surface of indicated *B. burgdorferi* strains. **(B)** The deposition of human or mouse MAC on the surface of *B. burgdorferi* were measured by flow cytometry and presented as mean fluorescence index ("MFI"). Each bar represents the mean of three independent determinations ± SEM. Significant differences ($p < 0.05$ by Kruskal-Wallis test with Dunn's multiple comparison) in the deposition levels of MAC relative to the strain B313 ("Φ") are indicated.

Figure S7. Untreated *B. burgdorferi* did not require CspZ to survive in human and quail serum. Untreated *B. burgdorferi* strain B31-A3 or B31-A3Δ*cspZ* harboring the vector pKFSS-1 ("B31-A3Δ*cspZ*/Vector") was incubated for four hours with untreated (filled bars) or heat-inactivated ("Heat-treated", hatched bars) serum at a final concentration of 40%. These sera include **(A)** normal human serum, **(B)** C3-depleted human serum ("Human $C3^-$ serum"), or **(C)** quail serum. The number of motile spirochetes was assessed microscopically. The percentage of surviving *B. burgdorferi* was calculated using the number of mobile spirochetes at four hours post incubation normalized to that immediately after incubation with serum. Each bar represents the mean of three independent determinations ± SEM. No significant differences ($p > 0.05$ by Kruskal-Wallis test with Dunn's multiple comparison) in the percentage survival of spirochetes relative to the strain B31-A3Δ*cspZ*/Vector were observed.

Figure S8. CspZ was not required to facilitate bacteremia and tissue colonization of untreated *B. burgdorferi* in mice. BALB/c mice were subcutaneously infected with 10^3 cells of untreated *B. burgdorferi* strain B31-A3 or B31-A3Δ*cspZ* harboring the vector pKFSS-1 ("Δ*cspZ*/Vector"). These mice were sacrificed at **(left panel)** 7 or **(right panel)** 14 days post-infection ("dpi"). The spirochete burdens in the **(A)** blood, **(B)** inoculation site of skin ("Inoc. Site"), **(C)** heart, **(D)** bladder, and **(E)** tibiotarsus joints were determined by qPCR and normalized to 1μg total DNA. Shown are the geometric mean ± geometric standard deviation of 5 mice per group. There were no significant differences ($p > 0.05$ by Mann-Whitney test) in the spirochete burdens between strains.

Figure S9. Dissemination of blood-treated *B. burgdorferi* in *Coturnix* quail. *Coturnix coturnix* quail were subcutaneously infected with 10^6 cells of human blood-treated *B. burgdorferi* strain B31-A3. At 3 and 7 days post-infection (dpi), the spirochete loads in the inoculation site of skin ("Inoc. Site"), blood, liver, heart, and brain were determined by qPCR and normalized to 1μg total DNA. Shown are the geometric mean of bacterial loads ± geometric standard deviation of 6 (for samples at 3dpi) or 8 (for samples at 7dpi) quail per group. Significant differences ($p < 0.05$; Mann-Whitney test) in colonization relative to 3 dpi are indicated ("*").

SUPLEMENTAL TABLES

Table S1. CspZ-Y207A/Y211A displayed undistinguishable levels of fibronectin, laminin, and plasminogen binding as WT CspZ.

Ligands	Recombinant CspZ proteins	K_D (μM)	P[a]
Fibronectin	GST-CspZ	1.16±0.01	0.15
	GST-CspZ-Y207A/Y211A	1.03±0.10	
	GST[b]	n.b.[c]	
Laminin	GST-CspZ	3.27±1.12	0.61
	GST-CspZ-Y207A/Y211A	3.89±1.64	
	GST	n.b.[c]	
Plasminogen	GST-CspZ	1.36±0.71	0.59
	GST-CspZ-Y207A/Y211A	1.88±1.36	
	GST	n.b.[c]	

All values represent the mean ± SEM of three experiments determined by ELISA.

[a] The statistical analysis of the K_D values derived from the binding of a particular ligand to GST-CspZ or GST-CspZ-Y207A/Y211A determined by Mann-Whitney test.

[b] GST was included as a negative control.

[c] No binding activity was detected.

Table S2. The viability of *B. burgdorferi* with no treatment or after treatment with human blood.

Strain	Percentage of live spirochetes	
	Untreated	Blood-treated
B31-A3	97.4±0.1[a]	90.4±0.5
ΔcspZ/pKFSS	97.9±0.2	95.1±0.2
pCspZ-B31	96.7±0.2	93.8±0.3
pCspZ-Y207A/Y211A	97.5±0.3	96.6±0.00

[a] The mean of live spirochetes percentage ± standard deviation of three samples per group.

Table S3. The generation time of untreated and human blood-treated *B. burgdorferi* strains used in this study.

Strain	Generation time (hour)[a]	
	Untreated	Blood-treated
B31-A3	15.8±2.1	17.5±1.2
ΔcspZ/pKFSS	15.8±2.3	17.5±0.4
pCspZ-B31	17.9±2.1	18.1±0.7
pCspZ-Y207A/Y211A	16.2±1.0	17.3±1.8

[a] The mean of generation time ± standard deviation of three samples per group.

1347 **Table S4. Primers used in this study.**

Primer	Sequence[a]	Amplified DNA fragment	Purpose
CSPZF-3	agacgctatttataacgaatgtacaggagc	*BBcspZ*	qRT-PCR quantification
CSPZR-4	cagcaacatgtctggcattagacac		
BBpCspZ_pKFSS-1_fp	gcGCATGCGcaatttttttaaaaaatat	*BBcspZ* promoter	For transforming shuttle vector
BBpCspZ_pKFSS-1_rp	gcGTCGACattttctcccctgctaaaat		
BBCspZ_pKFSS-1_fp	gcGTCGACatgaaaaaaagttttttat	*BBcspZ*	For transforming shuttle vector
BBCspZ_pKFSS-1_rp	gcGGATCCctataataaagtttgctta		
BBCspZ_prt_fp	gcGGATCCgatgttagtagattaaatc	BBCspZ AA residues 19-237	For transforming expression vector
BBCspZ_prt_rp	gcGTCGACctataataaagtttgctta		
Borrelia_16srRNAfp	gcttcgcttgtagatgagtctgc	*Borrelia 16s rRNA*	qRT-PCR control
Borrelia_16srRNArp	ttccagtgtgaccgttcacc		
BBRecAfp	gtggatctattgtattagatgaggctctcg	*BBrecA*	qRT-PCR control; qPCR spirochete burden
BBRecArp	gccaaagttctgcaacattaacacctaaag		
ColE1fp	ctacatacctcgctctgctaatc	pKFSS-1 origin of replication	PCR confirmation of transformation
ColE1rp	cgaaacccgacaggactataaa		
mNidfp	ccagccacagaatcccatcc	*mNidogen*	qPCR control
mNidrp	ggacatactctgctgccatc		
oIMR1325	atcttgagtgcaccaagcc	*mC3*	Genotyping BALB/c $C3^{-/-}$ mice
oIMR1326	ggttgcagcagtctatgaagg		
oIMR7415	gccagaggccacttgtgtag		
qß-actinfp	ctggcacctagcacaatgaa	qß-actin	qPCR control
qß-actinrp	ctgcttgctgatccacatct		

[a] Restriction sites used are shown in underlined capital letters

Fig. 1

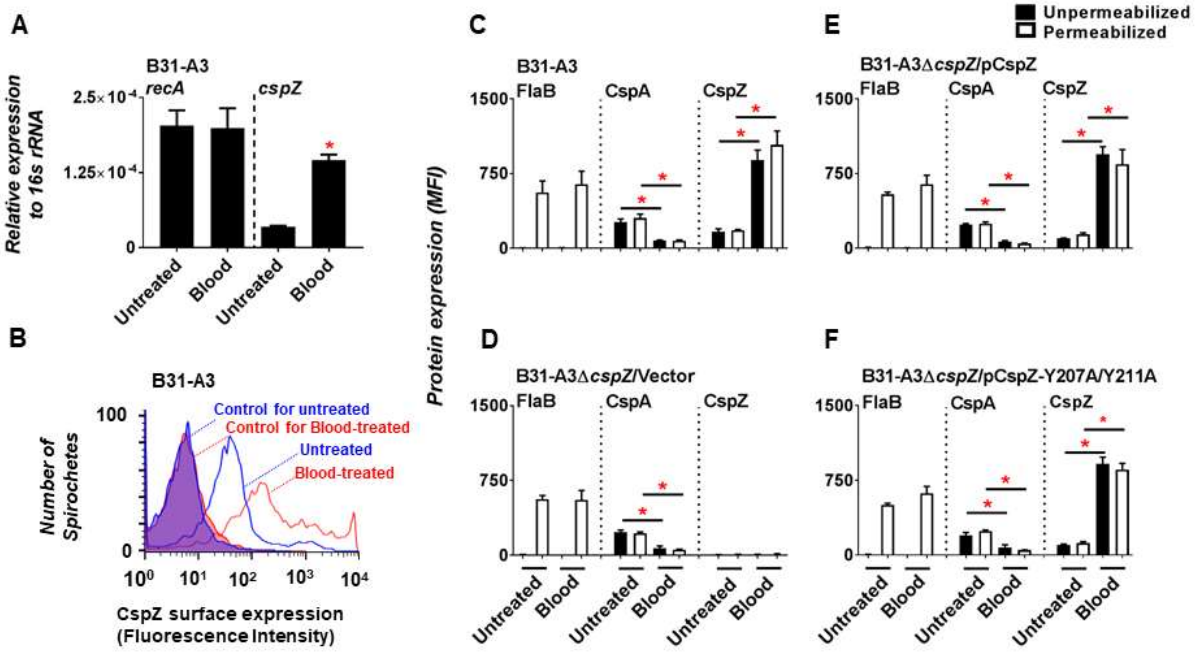
A
B31-A3
recA
cspZ
Relative expression to 16s rRNA
2.5×10⁻⁴
1.25×10⁻⁴
0
Untreated
Blood
Untreated
Blood
B
B31-A3
Number of Spirochetes
100
0
Control for untreated
Control for Blood-treated
Untreated
Blood-treated
10⁰ 10¹ 10² 10³ 10⁴
CspZ surface expression (Fluorescence Intensity)
Protein expression (MFI)
C
B31-A3
FlaB
CspA
CspZ
1500
750
0
D
B31-A3ΔcspZ/Vector
E
B31-A3ΔcspZ/pCspZ
F
B31-A3ΔcspZ/pCspZ-Y207A/Y211A
Unpermeabilized
Permeabilized

Fig. 2

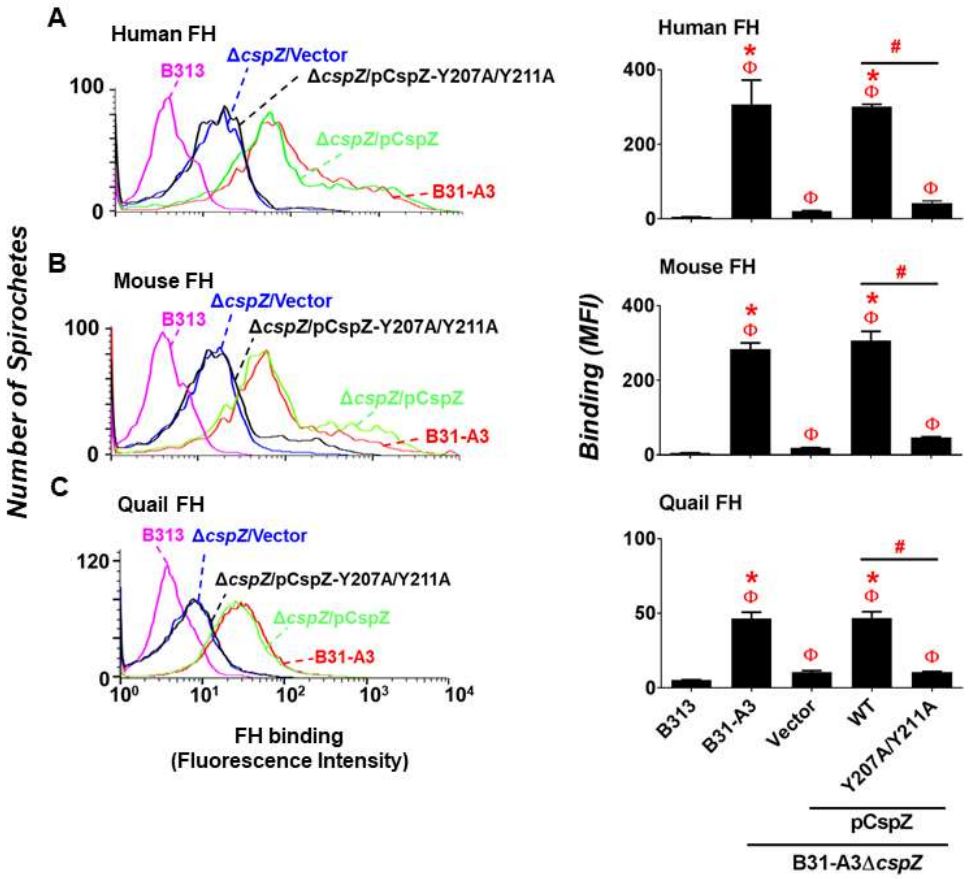
A
Human FH
B313
ΔcspZ/Vector
ΔcspZ/pCspZ-Y207A/Y211A
ΔcspZ/pCspZ
B31-A3
B
Mouse FH
C
Quail FH
Number of Spirochetes
FH binding
(Fluorescence Intensity)
Binding (MFI)
B313
B31-A3
Vector
WT
Y207A/Y211A
pCspZ
B31-A3ΔcspZ

Fig. 3

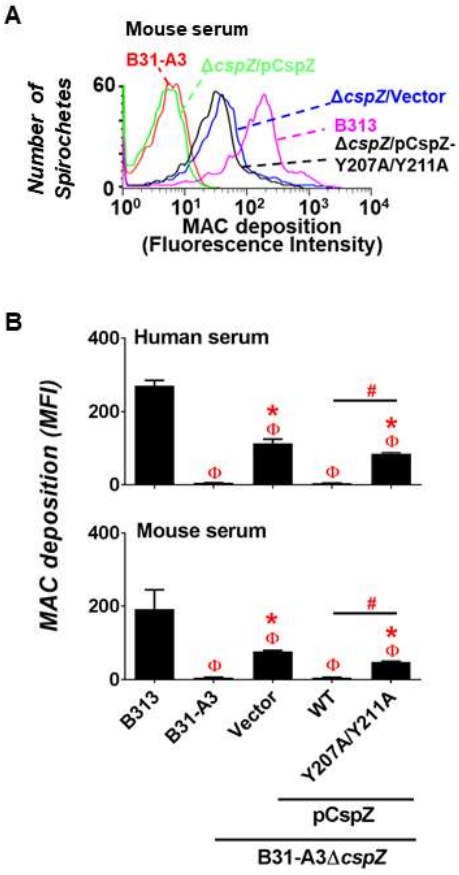
A
Mouse serum
B31-A3
ΔcspZ/pCspZ
ΔcspZ/Vector
B313
ΔcspZ/pCspZ-Y207A/Y211A
Number of Spirochetes
60
0
10^0
10^1
10^2
10^3
10^4
MAC deposition (Fluorescence Intensity)
B
MAC deposition (MFI)
400
200
0
Human serum
Mouse serum
#
*
Φ
B313
B31-A3
Vector
WT
Y207A/Y211A
pCspZ
B31-A3ΔcspZ

Fig. 4

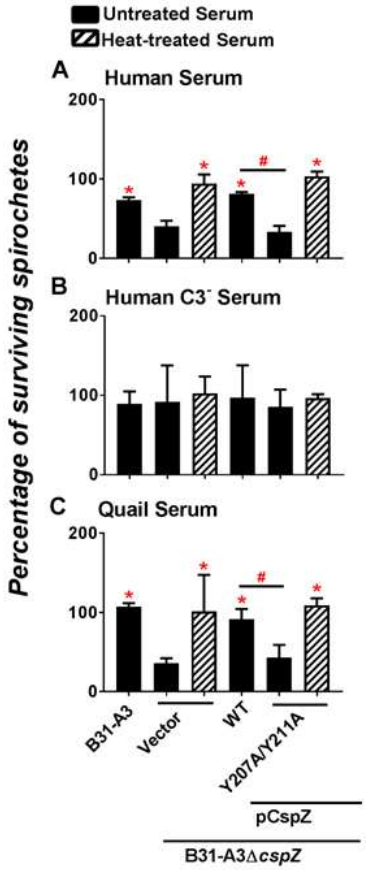
Untreated Serum
Heat-treated Serum
A
Human Serum
B
Human C3⁻ Serum
C
Quail Serum
Percentage of surviving spirochetes
200
100
0
*
#
B31-A3
Vector
WT
Y207A/Y211A
pCspZ
B31-A3Δ*cspZ*

Fig. 5

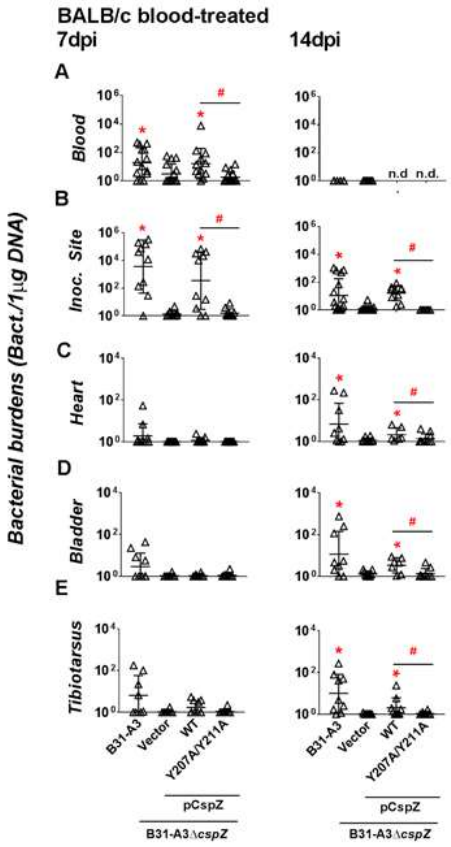
BALB/c blood-treated
7dpi
14dpi
A
Blood
B
Inoc. Site
C
Heart
D
Bladder
E
Tibiotarsus
Bacterial burdens (Bact./1μg DNA)
n.d
n.d.
B31-A3
Vector
WT
Y207A/Y211A
pCspZ
B31-A3Δ*cspZ*

Fig. 6

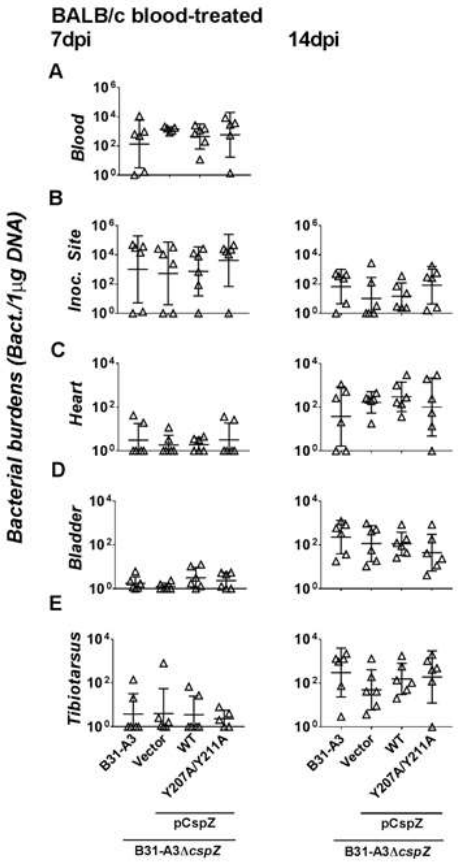
BALB/c blood-treated
7dpi
14dpi
A
B
C
D
E
Blood
Inoc. Site
Heart
Bladder
Tibiotarsus
Bacterial burdens (Bact./1μg DNA)
B31-A3
Vector
WT
Y207A/Y211A
pCspZ
B31-A3Δ*cspZ*

Fig. 7

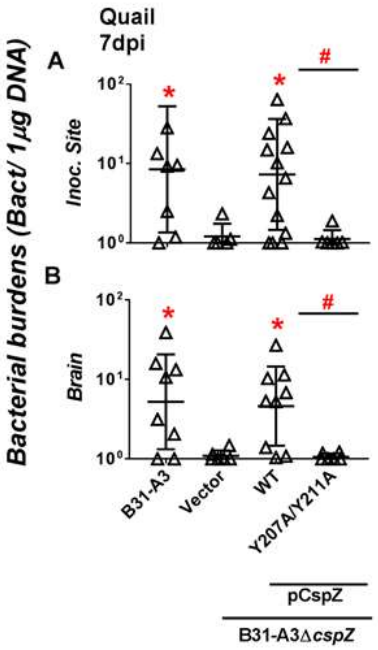
Quail
7dpi
A
B
Inoc. Site
Brain
Bacterial burdens (Bact/ 1μg DNA)
10^2
10^1
10^0
*
#
B31-A3
Vector
WT
Y207A/Y211A
pCspZ
B31-A3ΔcspZ

Fig. S1

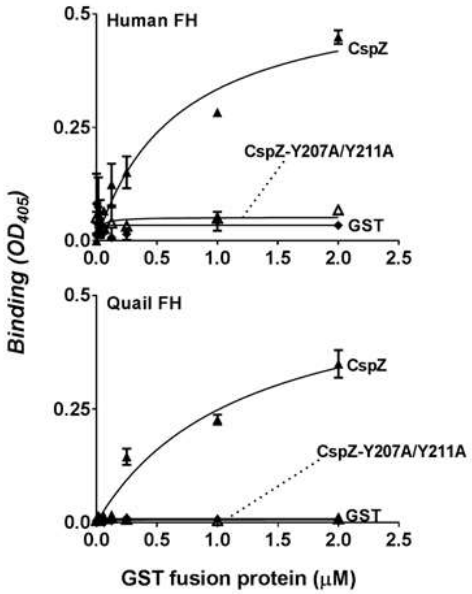
Human FH
CspZ
CspZ-Y207A/Y211A
GST
Quail FH
CspZ
CspZ-Y207A/Y211A
GST
Binding (OD405)
GST fusion protein (μM)
0.5
0.25
0.0
0.0
0.5
1.0
1.5
2.0
2.5

Fig. S2

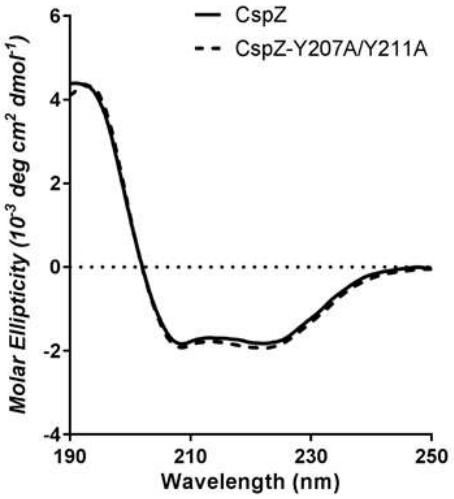
CspZ
CspZ-Y207A/Y211A
Molar Ellipticity (10^{-3} deg cm^2 $dmol^{-1}$)
6
4
2
0
-2
-4
190
210
230
250
Wavelength (nm)

Fig. S3

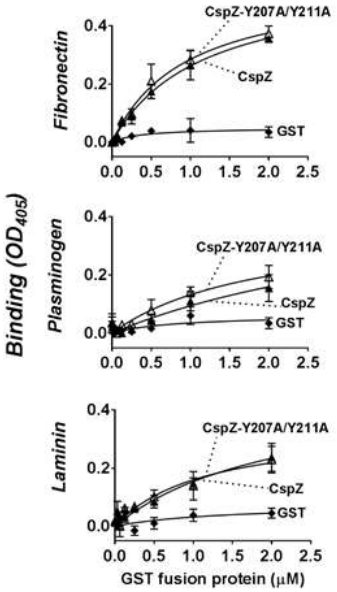
Binding (OD_{405})
Fibronectin
Plasminogen
Laminin
CspZ-Y207A/Y211A
CspZ
GST
0.0
0.2
0.4
0.0 0.5 1.0 1.5 2.0 2.5
GST fusion protein (μM)

Fig. S4

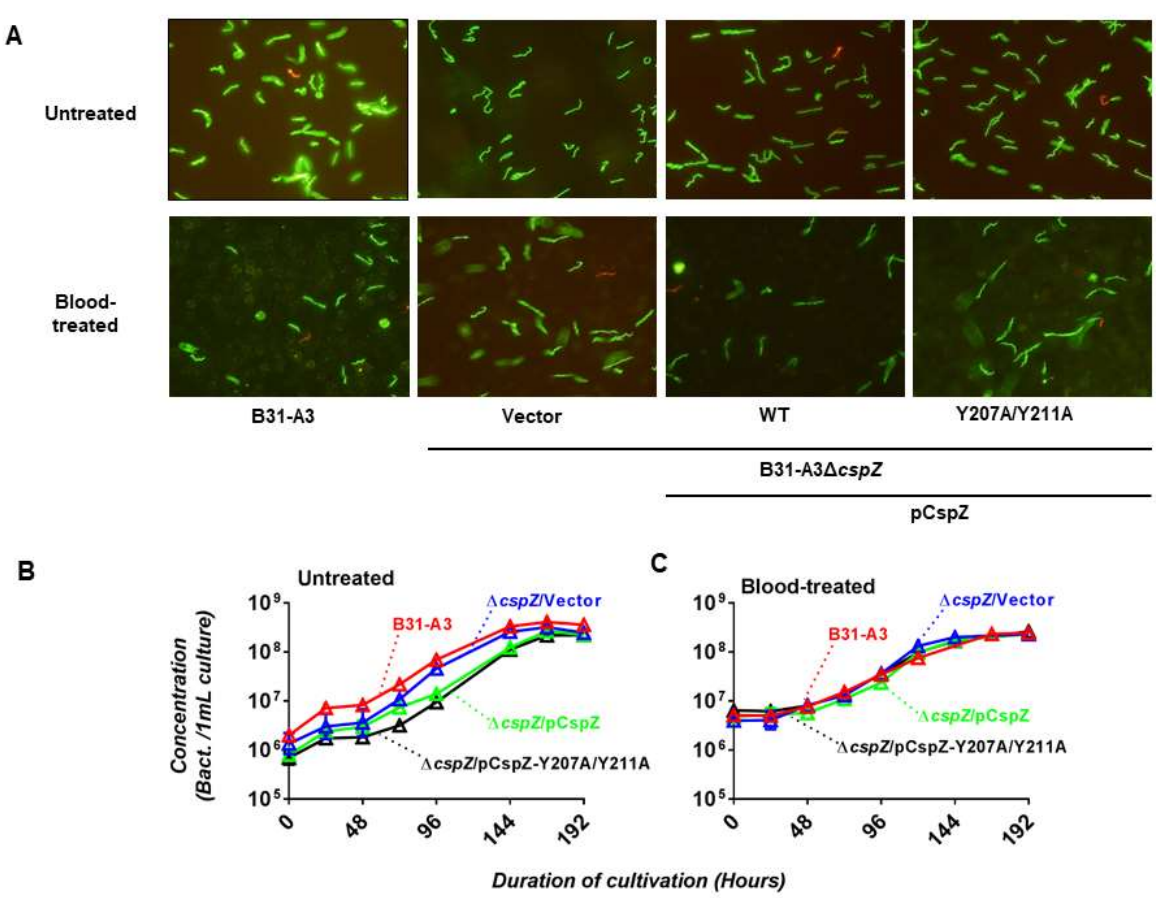
A
Untreated
Blood-treated
B31-A3
Vector
WT
Y207A/Y211A
B31-A3ΔcspZ
pCspZ
B
Untreated
ΔcspZ/Vector
B31-A3
ΔcspZ/pCspZ
ΔcspZ/pCspZ-Y207A/Y211A
Concentration (Bact. /1mL culture)
Duration of cultivation (Hours)
C
Blood-treated
ΔcspZ/Vector
B31-A3
ΔcspZ/pCspZ
ΔcspZ/pCspZ-Y207A/Y211A

Fig. S5

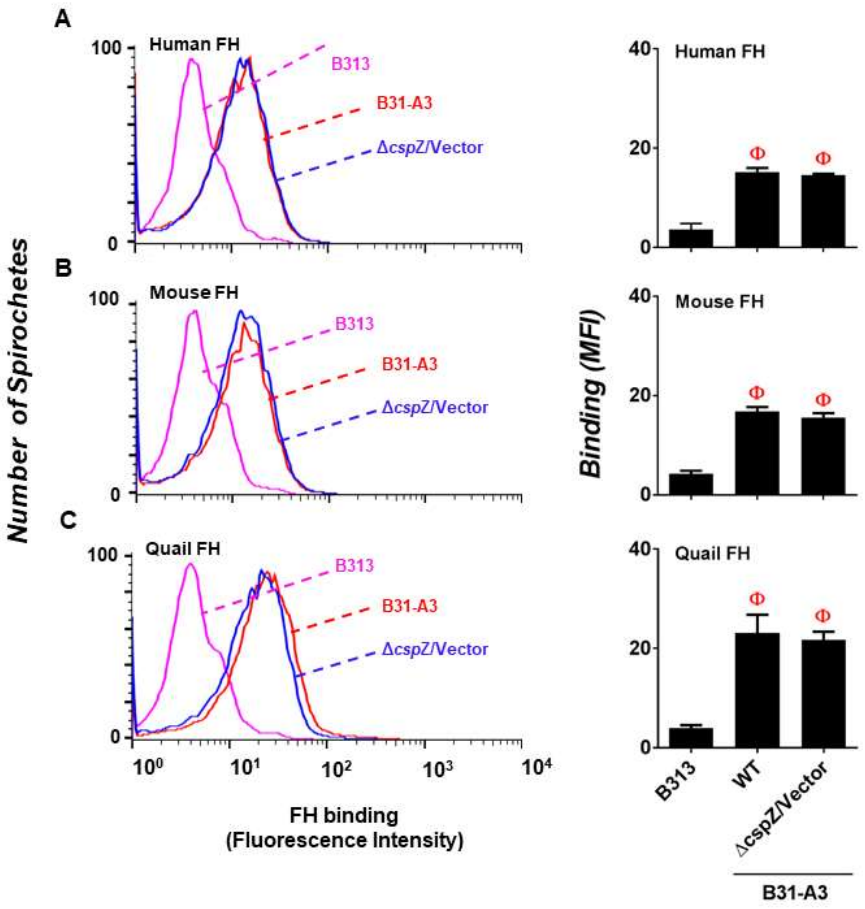
A
Human FH
B313
B31-A3
ΔcspZ/Vector
B
Mouse FH
C
Quail FH
Number of Spirochetes
FH binding
(Fluorescence Intensity)
Binding (MFI)
B313
WT
ΔcspZ/Vector
B31-A3

Fig. S6

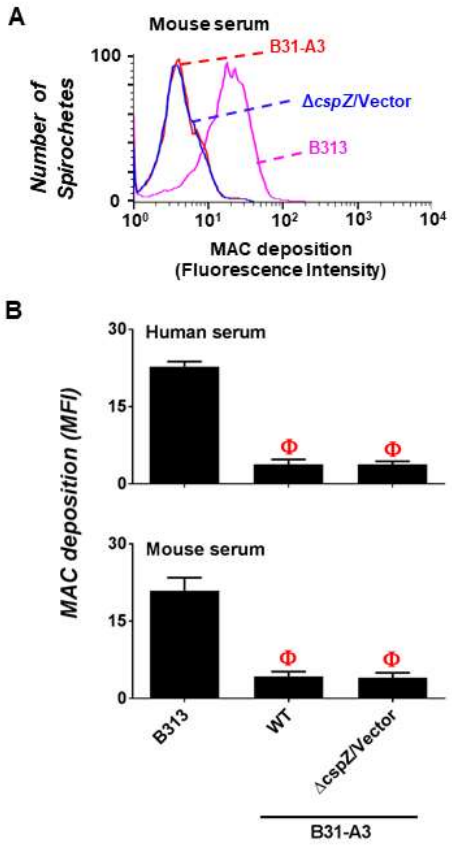
A
Mouse serum
B31-A3
ΔcspZ/Vector
B313
Number of Spirochetes
100
0
10^0
10^1
10^2
10^3
10^4
MAC deposition
(Fluorescence Intensity)
B
Human serum
Mouse serum
MAC deposition (MFI)
30
15
0
Φ
B313
WT
ΔcspZ/Vector
B31-A3

Fig. S7

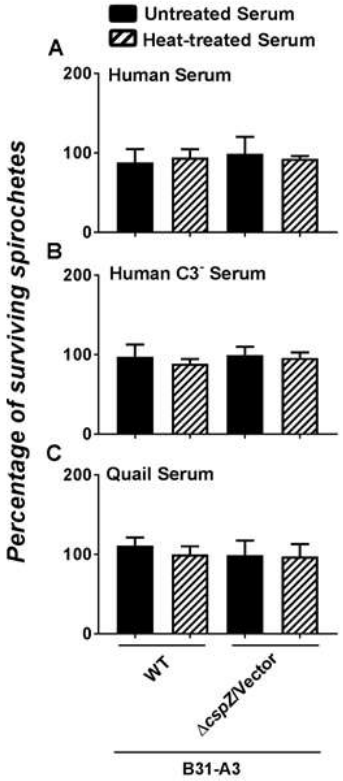
Untreated Serum
Heat-treated Serum
A
Human Serum
B
Human C3⁻ Serum
C
Quail Serum
200
100
0
Percentage of surviving spirochetes
WT
ΔcspZ/Vector
B31-A3

Fig. S8

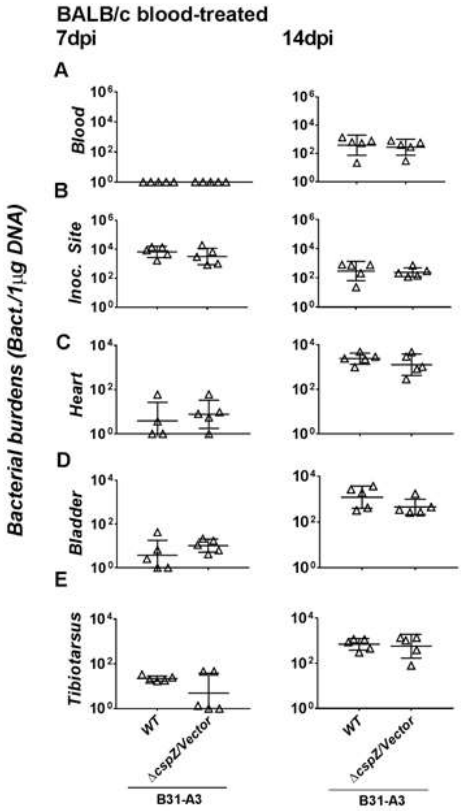
BALB/c blood-treated
7dpi
14dpi
A
Blood
B
Inoc. Site
C
Heart
D
Bladder
E
Tibiotarsus
Bacterial burdens (Bact./1μg DNA)
WT
ΔcspZ/Vector
B31-A3
WT
ΔcspZ/Vector
B31-A3

Fig. S9

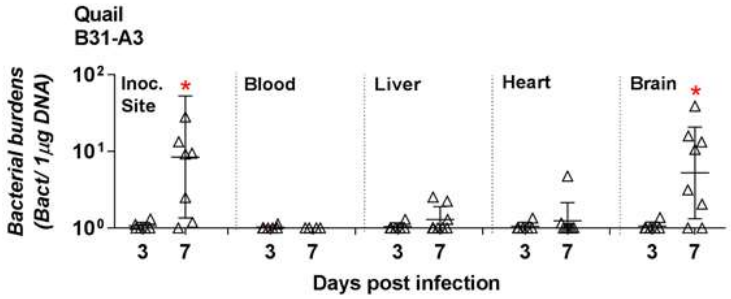
Quail
B31-A3
Bacterial burdens
(Bact/ 1μg DNA)
10²
10¹
10⁰
Inoc.
Site
Blood
Liver
Heart
Brain
*
*
3
7
3
7
3
7
3
7
3
7
Days post infection

1702